PalZ (2022) 96:449–469
https://doi.org/10.1007/s12542-021-00575-6

RESEARCH PAPER

Late Devonian–Mississippian conodont biostratigraphy of the Chelcheli section, NE Shahrud (Eastern Alborz, North Iran)

Ali Bahrami[1] · Peter Königshof[2] · Christoph Hartkopf-Fröder[3] · Sandra I. Kaiser[4]

Received: 29 September 2020 / Accepted: 20 July 2021 / Published online: 2 November 2021

Abstract

Devonian/Carboniferous conodonts from the Chelcheli section in the Alborz Mountains were investigated. Although conodonts are generally less abundant in the entire section, important zonal index taxa of the widely applied conodont standard zonation could be used for a precise conodont zonation. Forty-seven conodont species belonging to fifteen genera were identified and led to the discrimination of fifteen conodont zones, ranging from the *Palmatolepis minuta minuta* Zone into the *Scaliognathus anchoralis-Doliognathus latus* Zone. At the Devonian/Carboniferous boundary (DCB), characteristic lithologies such as black shales and massive sandstones represent equivalents of the Hangenberg Black Shale and Hangenberg Sandstone. Close to the DCB, there is a small stratigraphic hiatus in the conodont record which might be a result of facies (shallow-water succession with no conodont record and siliciclastic rocks) rather than a period of non-deposition as the sedimentological record seems continuous. Similar to other DCB sections in shallow-water facies in Iran the two biostratigraphically important species *Protognathodus kockeli* and *Protognathodus kuehni* do not occur.

Keywords Biostratigraphy · Devonian/Carboniferous boundary (DCB) · Eastern Alborz · Hangenberg crisis · Neritic facies

Introduction

The Alborz range in northern Iran is an active fold-and-thrust belt (Berberian 1983; Alavi 1996) and is situated about 200–500 km to the north of the Neo-Tethyan suture. The closure of the Palaeotethys between the Iran Plate as a part of Gondwana and the Turan Plate (Laurussia) occurred in the early Late Triassic and was accomplished during the Early/earliest Mid Jurassic (Golonka 2002). During the Palaeozoic, Iran was situated at the northern margin of Gondwana (Berberian and King 1981; Scotese 2001). In the mid-Palaeozoic, most of Iran was located about 20°–25° south of the palaeoequator. During the Mississippian, the Alborz Basin was positioned at a palaeolatitude of approximately 45–50° S (Vachard 1996; Torsvik and Cocks 2004, 2013; Muttoni et al. 2009). Devonian and Carboniferous rocks are most widespread in central and eastern Alborz but they belong to different structural units, some of which are separated by suture zones (Stöcklin 1968; Alavi 1991; Davoudzadeh 1997). The most important structural units in Iran are summarized in Fig. 1. During the last decades, a number of sections in eastern Alborz were studied due to their high fossil content and excellent preservation (e.g. Bozorgnia 1973; Brice et al. 1974; Ahmadzadeh-Heravi 1975; Jenny 1977;

Handling Editor: Mike Reich.

✉ Ali Bahrami
a.bahrami@sci.ui.ac.ir; Bahrami_geo@yahoo.com

Peter Königshof
peter.koenigshof@senckenberg.de

Christoph Hartkopf-Fröder
hartkopf-froeder@gd.nrw.de

Sandra I. Kaiser
dr.sandra.kaiser@gmail.com

[1] Department of Geology, Faculty of Sciences, University of Isfahan, Isfahan, Iran

[2] Senckenberg, Research Institute and Natural History Museum, Senckenberganlage 25, 60325 Frankfurt am Main, Germany

[3] Geological Survey NRW, De-Greiff-Str. 195, 47803 Krefeld, Germany

[4] State Museum of Natural History Stuttgart, Rosenstein 1, 70191 Stuttgart, Germany

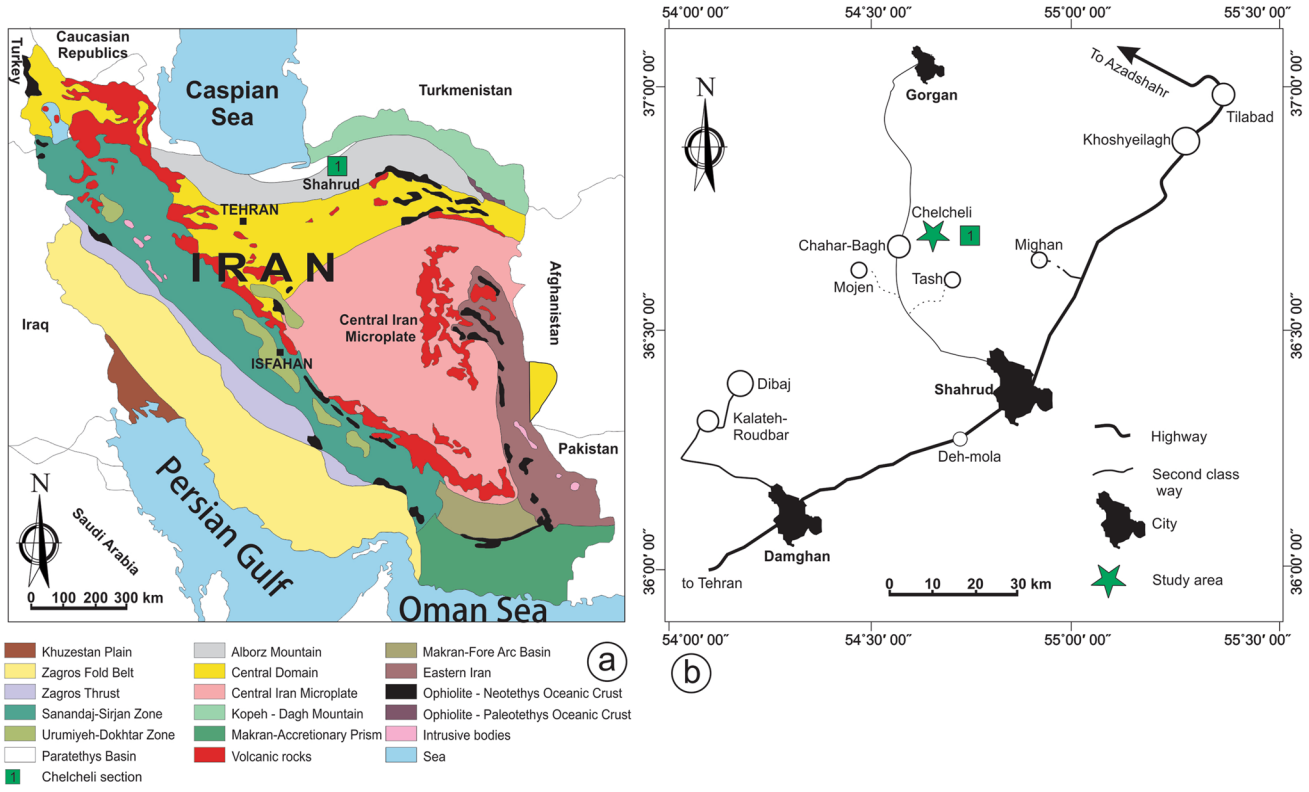

Fig. 1 **a** Structural units of Iran and position of Chelcheli section, near Shahrud and Chahar-Bagh village; **b** topographic map of the area, the asterisk shows the position of the section

Coquel et al. 1977; Ashouri 1990, 2006; Wendt et al. 2005; Ghavidel-Syooki and Owens 2007; Hashemi 2011; Falahatgar and Mosaddegh 2012; Falahatgar et al. 2018; Abadi et al. 2015, 2017; Pour et al. 2018; Valeryi et al. 2018; Parvizi et al. 2021). Recently, Devonian/Carboniferous boundary (DCB) sections became a focus of international research (Aretz et al. 2013; Corradini et al. 2016). First results on DCB sections in Iran are shortly summarized in Königshof et al. (2021). The fundamental importance to study this interval is linked with one of the major extinction events (Hangenberg Crisis) in Earth's history. Based on the ecological severity index by McGhee et al. (2013) the end-Devonian extinction is known as the seventh severe mass extinction in Phanerozoic. This first-order mass extinction eliminated nearly 20% of marine invertebrate genera and reduced the long-term biodiversity of all vertebrates by about 50% (Sepkoski 1996; Walliser 1996; Sandberg et al. 2002). The D/C transition is characterized by several transgressive/regressive cycles and widespread ocean anoxia have been recognized along continental margins or epicontinental basins known as the Hangenberg Black Shale Event (HBS). Close to the DCB a major sea-level fall (Hangenberg Sandstone Event, HSS) of assumed more than 100 m (Kaiser et al. 2011; Myrow et al. 2014 see review summary in Kaiser et al. 2016) which is associated with the glaciation on Gondwana (e.g. Isaacson et al. 1999, 2008; Streel et al. 2000, 2001; Caputo et al. 2008; Brezinski et al. 2010; Lakin et al. 2016) can be recognized in many sections around the world. The deposition of these black shales and sandstones is known as the early and middle phase of the Hangenberg Crisis as defined by Kaiser et al. (2016) and Becker et al. (2016). Depending on facies setting equivalents of the regressive Hangenberg Sandstone can also be recognized as an unconformity and/or reworked sediments (see; Cole et al. 2015; Bábek et al. 2016; Kaiser et al. 2016). Stratigraphical gaps and non-deposition related to this major regression are also known from eastern Iran as it was shown by Bahrami et al. (2011). It is noteworthy that most DCB sections worldwide are described from hemipelagic and pelagic successions. To get a more comprehensive picture of one of the most interesting time slices in Earth's history it is necessary to study DCB sections in different depositional settings such as in shallow-water environments. Most of the DCB sections from the central and eastern Alborz Mountains have been deposited in a shallow-water, carbonate ramp setting (Königshof et al. 2021). However, in contrast to other DCB sections in Iran (Habibi et al. 2008; Bahrami et al. 2011), the Chelcheli section exhibits "characteristic rock" types around the DCB such as black shale and sandstone. In this study, we have sampled conodonts from the Khoshyeilagh Formation and the overlying Mobarak

Formation of the Chelcheli section with a special focus on the DCB. Herein, we present an improved conodont-based stratigraphical record around the DCB in neritic facies which is an important contribution to the ongoing discussion about a potential new definition of the DCB.

Geological setting and study area

Several sections in the eastern Alborz have repeatedly been studied in the past and have contributed considerably to the knowledge of the sedimentary record of the Devonian/Mississippian in northern Iran (e.g. Bozorgnia 1973; Brice et al. 1974, 1978; Stampfli 1978; Hamdi and Janvier 1981; Weddige 1984; Ashouri 1990, 1994, 2006; Ghavidel-Syooki 1994; Königshof et al. 2021). For the present study, we examined the Chelcheli section with a focus around the DCB. The section (Figs. 1 and 2) is located close to the Chahar-Bagh village of the Chelcheli Wildlife conservation area at the northern end of the N–S striking Chelcheli mountain range (about 70 km northwest of Shahrud city between Shahrud and Gorgan, sheet H4 Gorgan, 1: 250.000, see Salehirad et al. (1991); WGS coordinates: base of the section: 36° 36′ 15.54″ N; 54° 32′ 55.57″ E, top of the section: 36° 36′ 15.89″ N; 54° 32′ 48.49″ E).

The Chelcheli section is exposed along a steep cliff in the higher mountain range and has a thickness of about 1300 m. Rocks are mainly composed of neritic sediments of Mid-Devonian to Pennsylvanian age. This conodont study deals with samples from the Khoshyeilagh Formation and the overlying Mobarak Formation with a special focus on the DCB (Fig. 3a). Both formations are widely distributed in central and eastern parts of the Alborz Mountains and were studied intensively in the last decades due to their rich fossil content. However, there are still some uncertainties as detailed (bio-) stratigraphic investigations on the Khoshyeilagh Formation are still lacking (e.g. Bozorgnia 1973; Ashouri 1990, 1994, 2006).

The Khoshyeilagh Formation is mainly composed of limestone, shale and marl and thick-bedded sandstone close to the DCB. In the central Alborz Mountains, the Mobarak Formation conformably overlies the Upper Devonian Jeirud Formation (Abadi et al. 2015). This formation is an equivalent to the Upper Devonian Khoshyeilagh Formation in eastern Alborz Mountains (Königshof et al. 2021: fig. 8). In the Chelcheli section, the Mobarak Formation conformably overlies the Khoshyeilagh Formation. Whereas the base of this formation is defined, the top of the formation varies in age from the Tournaisian–early Visean? in the southern part of the Alborz Mountains to late Visean in the northern part of the Alborz Mountains (Bozorgnia 1973; Wendt et al.

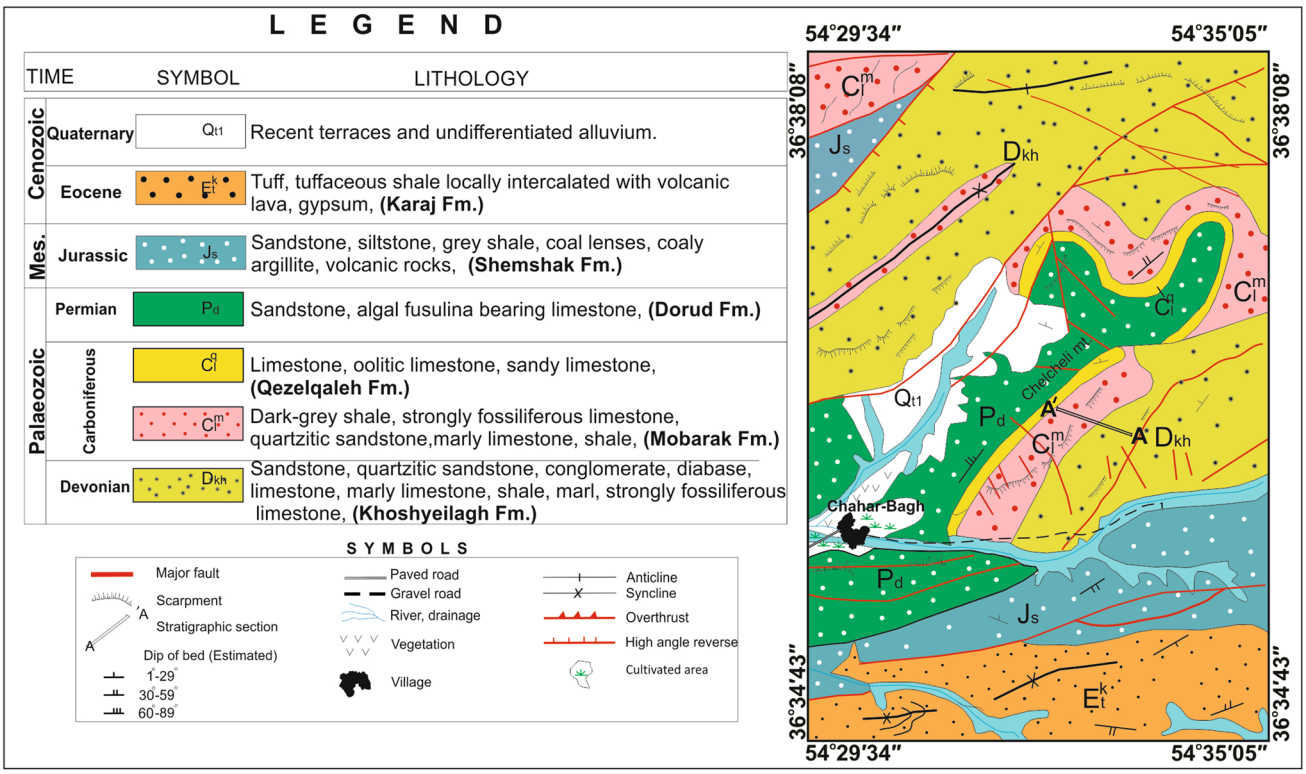

Fig. 2 Geological map of the area around the Chelcheli section (simplified after Salehirad et al. 1991)

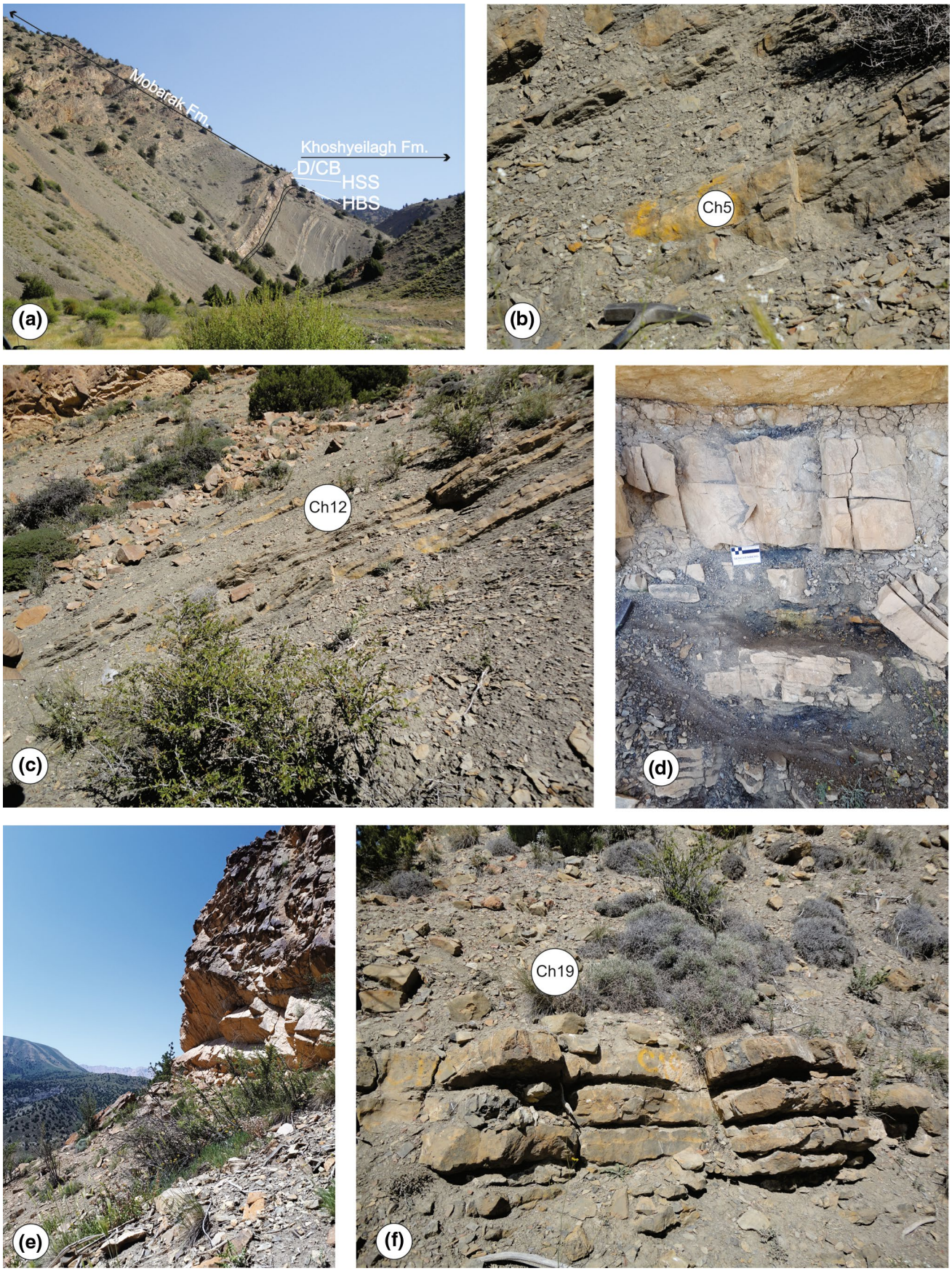
Mobarak Fm.
Khoshyeilagh Fm.
D/CB
HSS
HBS
(a)
Ch5
(b)
Ch12
(c)
(d)
(e)
Ch19
(f)

◂**Fig. 3** **a** Panoramic view of the Chelcheli section in eastern Alborz mountains; **b** grey shale and thin-bedded limestone at the base of Unit 2 (sample area Ch5); **c** dark-grey shale corresponds to the interval of the Dasberg Crisis within the *Bispathodus aculeatus aculeatus* conodont Zone (Unit 3, sample Ch12); **d** black shale layers and intercalated fine-grained sandstones equivalent to the black shales of the Hangenberg Black Shale Event (Unit 4, photo taken directly below the massive sandstone); **e** panoramic view of the black shales equivalent to the Hangenberg Black Shale and the overlying 10 m thick coarsening upward sandstone succession (equivalent to the Hangenberg Sandstone, Unit 5); **f** alternation of shales and carbonates at the beginning of the Early Mississippian carbonate cycle (Mobarak Formation, Unit 6 and 7)

2005; Brenckle et al. 2009). The age discrepancy might be a result of variable uplift across the southern Alborz Mountains during the late Visean until the Cisuralian (Bozorgnia 1973; Lasemi 2001; Wendt et al. 2005) and/or by a progressive drop in sea level linked to glacial episodes between the latest Visean–Serpukhovian and early Moscovian (Fielding et al. 2008; Haq and Schutter 2008; Rygel et al. 2008; Brenckle et al. 2009). The characteristic sediments of this formation are dark grey shale and thin-bedded limestone in the lower parts, which grade into thick to massively bedded limestones with abundant skeletal and non-skeletal fragments in the upper parts (Mosaddegh 2000; Lasemi 2001; Fig. 3). According to several authors (e.g. Webster et al. 2003, 2011; Torsvik and Cocks 2004; Wendt et al. 2005; Golonka 2007; Bagheri and Stampfli 2008; Brenckle et al. 2009) the Mobarak Formation represents the most extensive carbonate cycle along the northern margin of Gondwana which was deposited after the Palaeo-Tethys rift opening.

Lithology of the section

The Khoshyeilagh Formation of the Chelcheli section is 182 m thick and was subdivided into five lithological units (Figs. 3 and 4). The lowermost succession (Unit 1, samples Ch1–Ch4-1, thickness 37 m) contains black thin to medium-bedded limestone, with intercalated shale and marl layers. This unit is very fossiliferous and contains trilobites, brachiopods, gastropods, and micro-vertebrate remains. The overlaying unit (Unit 2, samples Ch5–Ch9-1, thickness

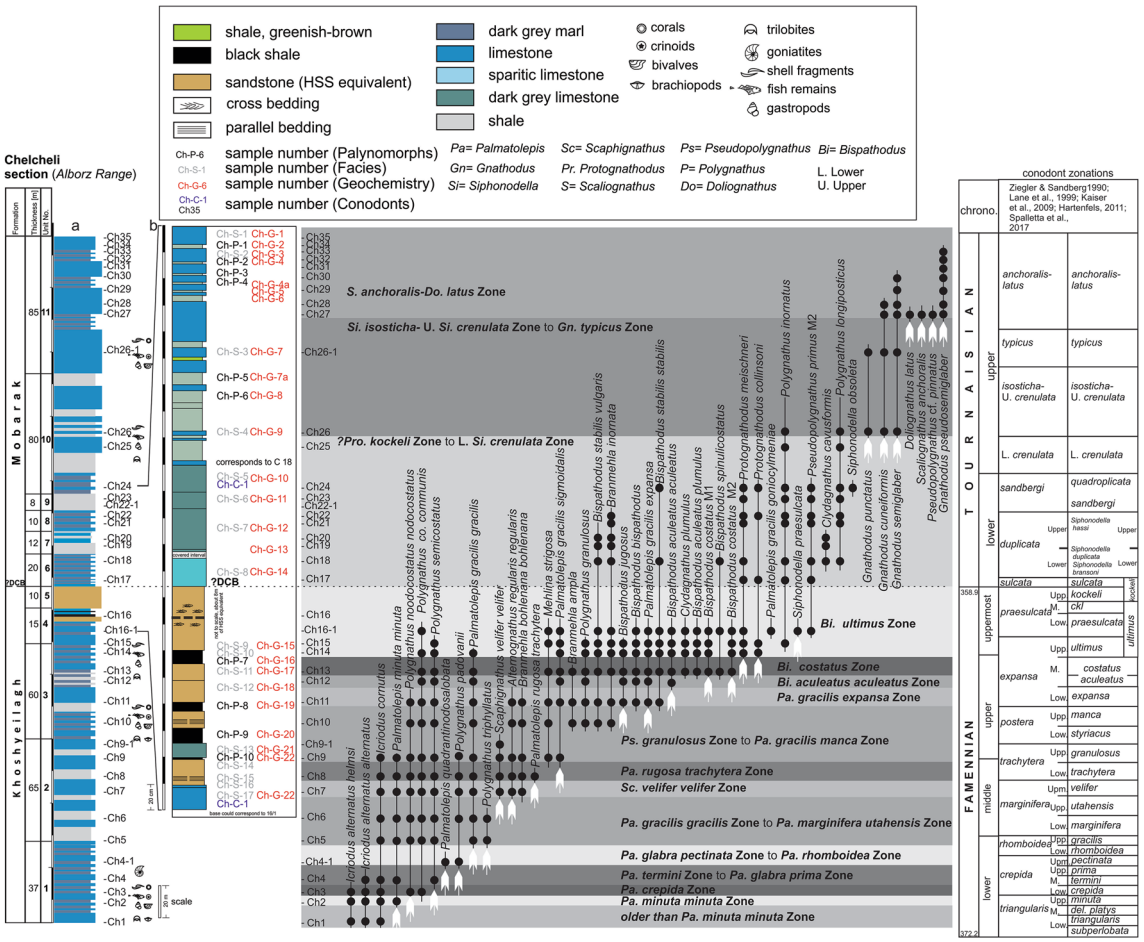

Fig. 4 Measured columnar section a and b with a special focus on the DC transition (section b), lithology, and conodont distribution of the Chelcheli section. The right columns show the conodont standard zonations of different authors (for explanation see text)

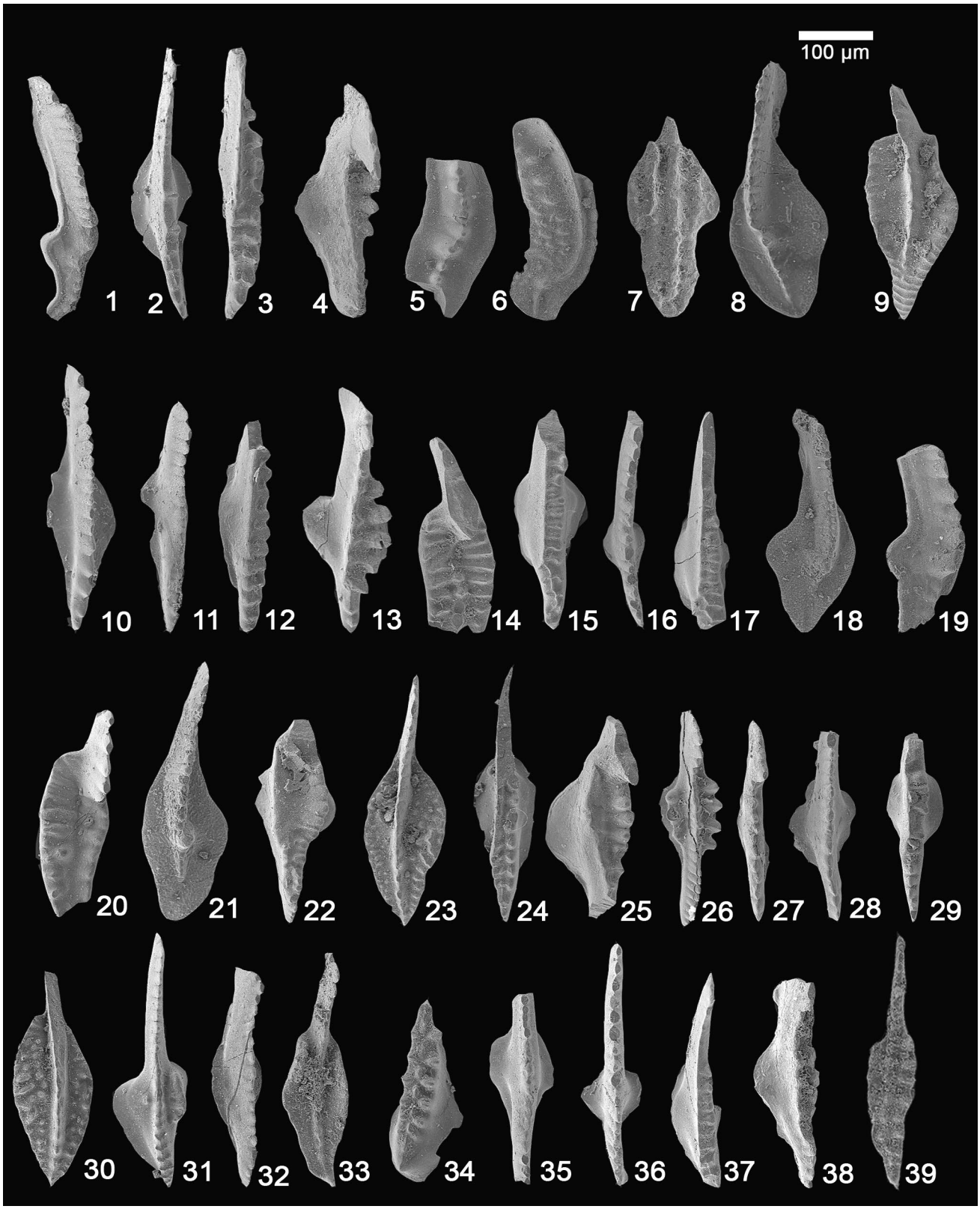
100 µm
1
2
3
4
5
6
7
8
9
10
11
12
13
14
15
16
17
18
19
20
21
22
23
24
25
26
27
28
29
30
31
32
33
34
35
36
37
38
39

◂**Fig. 5** Conodonts from the Chelcheli section, the scale bar is 100 µm. (1) *Palmatolepis gracilis sigmoidalis* Ziegler, 1962; Upper view of IUMC 723, sample Ch11. (2) *Bispathodus aculeatus aculeatus* (Branson and Mehl, 1934); Upper view of IUMC 724, sample Ch14. (3) *Bispathodus costatus* (Branson, 1934) Morphotype 2; Upper view of IUMC 725, sample Ch14. (4) *Clydagnathus plumulus* (Rhodes et al., 1969); Upper view of IUMC 726, sample Ch15. (5) *Palmatolepis* sp. Upper view of IUMC 727, sample Ch10. (6) *Palmatolepis rugosa trachytera* Ziegler, 1960; Upper view of IUMC 728, sample Ch8, X 150. (7) *Polygnathus triphyllatus* Helms, 1961; Upper view of IUMC 729, sample Ch8. (8) *Palmatolepis minuta minuta* Branson and Mehl, 1934; Upper view of IUMC 730, sample Ch4. (9) *Polygnathus semicostatus* Branson and Mehl, 1934 Morphotrend 3 sensu Dreesen and Orchard (1974); Upper view of IUMC 731, sample Ch15. (10) *Bispathodus stabilis stabilis* (Branson and Mehl, 1934); Upper view of IUMC 732, sample Ch15. (11) *Bispathodus stabilis stabilis* (Branson and Mehl, 1934); Upper view of IUMC 733, sample Ch16-1. (12) *Bispathodus jugosus* (Branson and Mehl, 1934); Upper view of IUMC 734, sample Ch15. (13) *Clydagnathus plumulus* Rhodes et al., 1969; Upper view of IUMC 735, sample Ch15. (14) *Scaphignathus velifer velifer* Helms, 1959; Upper view of IUMC 736, sample Ch9. (15) *Bispathodus spinulicostatus* (Branson, 1934) Morphotyp 1; Upper view of IUMC 737, sample Ch13. (16) *Branmehla inornata* (Branson and Mehl, 1934); Upper view of IUMC 738, sample Ch18. (17) *Bispathodus spinulicostatus* (Branson, 1934) Morphotyp 1; Upper view of IUMC 739, sample Ch18. (18) *Palmatolepis minuta minuta* Branson and Mehl, 1934; Upper view of IUMC 740, sample Ch6. (19) *Palmatolepis gracilis sigmoidalis* Ziegler, 1962; Upper view of IUMC 741, sample Ch13. (20) *Scaphignathus velifer velifer* Helms, 1959; Upper view of IUMC 742, sample Ch7. (21) *Palmatolepis minuta minuta* Branson and Mehl, 1934; Upper view of IUMC 743, sample Ch7. (22) *Clydagnathus cavusformis* Rhodes et al., 1969; Upper view of IUMC 744, sample Ch18. (23) *Polygnathus granulosus* Branson and Mehl, 1934; Upper view of IUMC 745, sample Ch15. (24) *Bispathodus jugosus* (Branson and Mehl, 1934); Upper view of IUMC 746, sample Ch12. (25) *Clydagnathus plumulus* (Rhodes et al., 1969); Upper view of IUMC 747, sample Ch13. (26) *Pseudopolygnathus primus* M2 Branson and Mehl, 1934; Upper view of IUMC 748, sample Ch24. (27) *Pandorinellina insita* Müller, 1956; Upper view of IUMC 749, sample Ch10. (28) *Bispathodus stabilis vulgaris* (Dzik, 2006); Upper view of IUMC 750, sample Ch18. (29) *Bispathodus spinulicostatus* (Branson, 1934) Morphotyp 1; Upper view of IUMC 751, sample Ch16-1. (30) *Polygnathus granulosus* Branson and Mehl, 1934; Upper view of IUMC 752, sample Ch14. (31) *Gnathodus semiglaber* Bischoff, 1957; Upper view of IUMC 753, sample Ch30. (32) *Bispathodus stabilis vulgaris* (Dzik, 2006); Upper view of IUMC 754, sample Ch14. (33) *Polygnathus communis communis* (Branson and Mehl, 1934); Upper view of IUMC 755, sample Ch13. (34) *Icriodus alternatus alternatus* Branson and Mehl, 1934 Morphotyp 1; Upper view of IUMC 756, sample Ch1. (35) *Bispathodus stabilis vulgaris* (Dzik, 2006); Upper view of IUMC 757, sample Ch18. (36) *Branmehla inornata* (Branson and Mehl, 1934); Upper view of IUMC 758, sample Ch19. (37) *Bispathodus costatus* (Branson, 1934) Morphotyp 2; Upper view of IUMC 759, sample Ch16-1. (38) *Bispathodus aculeatus aculeatus* (Branson and Mehl, 1934); Upper view of IUMC 760, sample Ch15. (39) *Alternognathus regularis regularis* Ziegler and Sandberg, 1984; Upper view of IUMC 761, sample Ch15

65 m) is mainly composed of shale, marl, and medium-bedded limestone. This succession is overlain by thin-bedded limestone followed by alternating medium-bedded limestone with dark-grey shale and marl (Unit 3, samples Ch10–Ch14, thickness 60 m). Distinct horizons, rich in brachiopods (samples Ch10–Ch11), occur in the middle part of this unit. Furthermore, based on both the conodont stratigraphy (*Bispathodus aculeatus aculeatus* Zone) as well as the lithology of the rocks (dark-grey shales) the interval around sample Ch12 may correspond to the interval of the Late Devonian Dasberg Crisis (compare Hartenfels 2011). Unit 4 (samples Ch15–Ch16, thickness 15 m) is composed of thick shale layers with alternating thin-bedded limestone and a very thin sandstone layer. Frequently, brachiopods and corals occur in some distinct horizons. Interestingly, the black shale represents not one single layer but is composed of three layers of several cm thickness (see Fig. 3d). This succession is covered by a massive quartzitic, coarsening-upward sandstone sequence of about 10 m thickness (Unit 5). The sediments of Unit 4 and Unit 5 are most probably equivalent to the Drewer Sandstone (regressive Hangenberg prelude episode) with intercalated transgressive black shale layers equivalent to the transgressive Hangenberg Black Shale (HBS) and finally the overlying regressive Hangenberg Sandstone (HSS). The Khoshyeilagh Formation is continuously overlain by the Lower Mississippian Mobarak Formation (thickness 215 m) which is composed of an alternation of nodular medium-bedded limestone and shale. This interval is less fossiliferous and only a limited number of macrofossils such as gastropods and brachiopods were found (Unit 6, samples Ch17–Ch18, thickness 20 m). The overlying unit exhibits green thick shale with some limestone layers (Unit 7, samples Ch19–Ch20, thickness 12 m). The succession grades upwards into thin-bedded limestone (Unit 8, samples Ch21–Ch22, thickness 10 m) which is covered by shale and thin limestone (Unit 9, sample Ch22-1–Ch23, thickness 8 m). This unit yielded only some conodonts (Fig. 4). The uppermost part of the Chelcheli section was subdivided into two units (Unit 10, samples Ch24–Ch26 and Unit 11, samples Ch26-1–Ch35) which have a thickness of 165 m. This succession is composed of an alternation of limestone (nodular and thin-bedded), shale and marl. Some distinct horizons are very fossiliferous and contain bivalves, trilobites, gastropods, fish remains, and corals.

Materials and methods

Thirty-nine conodont samples of approximately 4–5 kg each were taken from carbonate rock and processed by standard processing methods (see Jeppsson and Anehus (1995)). The overall number of conodont elements is relatively low as it was shown in other shallow-water sections for instance by Bahrami et al. (2018, 2019), Munkhjargal et al. (2021) and Königshof et al. (2021). However, a total of 338 conodonts were obtained from the residues of which a reasonable number of species is biostratigraphically important. The conodont collection is stored at the Department of Geology

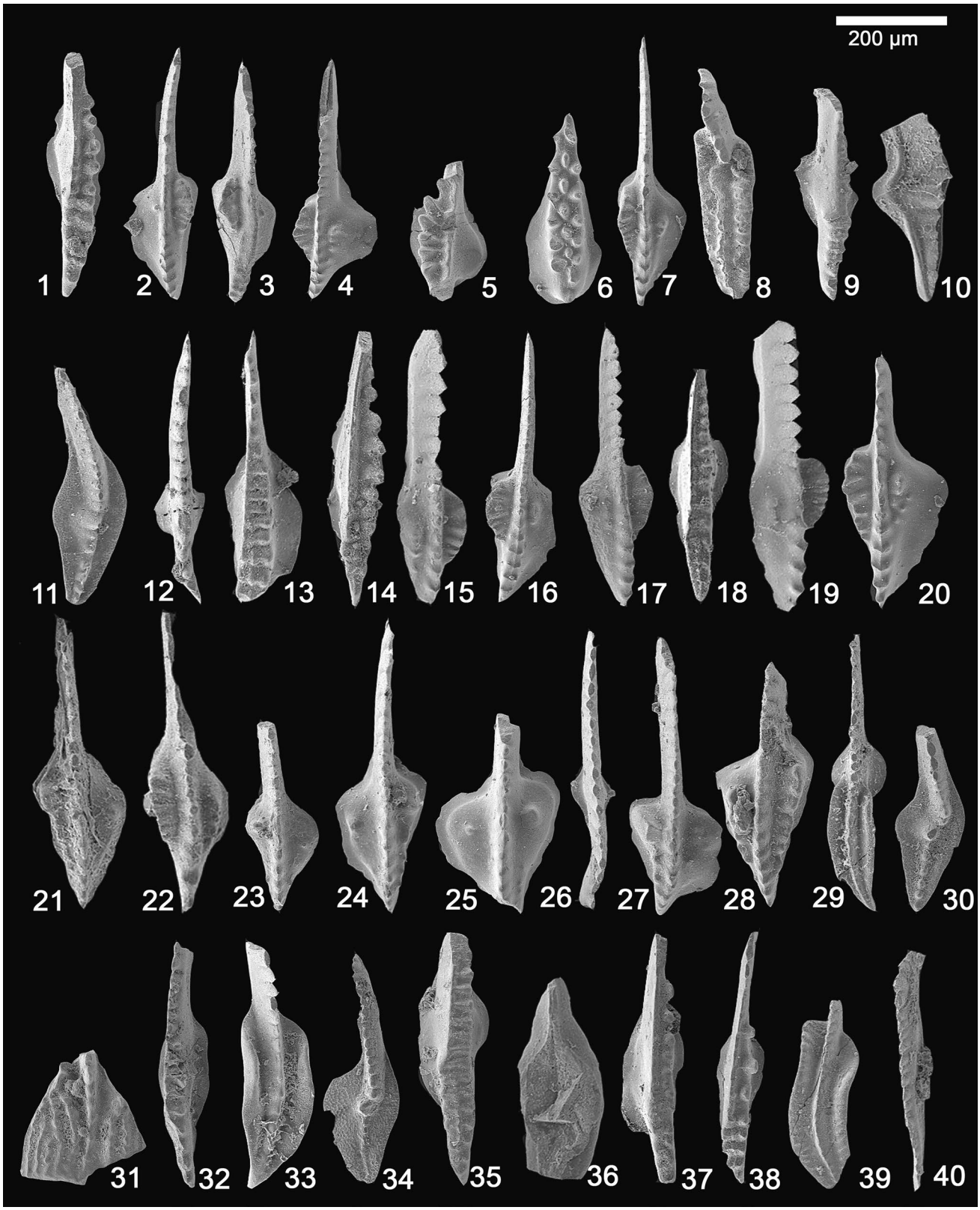
200 µm
1
2
3
4
5
6
7
8
9
10
11
12
13
14
15
16
17
18
19
20
21
22
23
24
25
26
27
28
29
30
31
32
33
34
35
36
37
38
39
40

◂**Fig. 6** Conodonts from the Chelcheli section, the scale bar is 200 µm. (1) *Bispathodus jugosus* (Branson and Mehl, 1934); Upper view of IUMC 762, sample Ch11. (2) *Gnathodus semiglaber* Bischoff, 1957; Upper view of IUMC 763, sample Ch26. (3) *Gnathodus semiglaber* Bischoff, 1957; Upper view of IUMC 764, sample Ch26-1. (4) *Gnathodus pseudosemiglaber* Thompson and Fellows, 1970; Upper view of IUMC 765, sample Ch35. (5) *Clydagnathus plumulus* Rhodes et al., 1969; Upper view of IUMC 766, sample Ch13. (6) *Icriodus alternatus helmsi* Sandberg and Dreesen, 1984; Upper view of IUMC 767, sample Ch3. (7) *Gnathodus pseudosemiglaber* Thompson and Fellows, 1970; Upper view of IUMC 768, sample Ch28. (8) *Scaphignathus velifer velifer* Helms, 1959; Upper view of IUMC 769, sample Ch8. (9) *Bispathodus jugosus* (Branson and Mehl, 1934); Upper view of IUMC 770, sample Ch12. (10) *Palmatolepis gracilis gracilis* Branson and Mehl, 1934; Upper view of IUMC 771, sample Ch9. (11) *Palmatolepis gracilis expansa* Sandberg and Ziegler, 1979 Morphotyp 1; Upper view of IUMC 772, sample Ch15. (12) *Branmehla inornata* (Branson and Mehl, 1934); Upper view of IUMC 773, sample Ch15. (13) *Bispathodus jugosus* (Branson and Mehl, 1934); Upper view of IUMC 774, sample Ch14. (14) *Bispathodus costatus* (Branson, 1934) Morphotyp 2; Upper view of IUMC 775, sample Ch14. (15) *Gnathodus pseudosemiglaber* Thompson and Fellows, 1970; Upper view of IUMC 776, sample Ch34. (16) *Gnathodus pseudosemiglaber* Thompson and Fellows, 1970; Upper view of IUMC 777, sample Ch33. (17) *Gnathodus pseudosemiglaber* Thompson and Fellows, 1970; Upper view of IUMC 778, sample Ch31. (18) *Bispathodus jugosus* (Branson and Mehl, 1934); Upper view of IUMC 779, sample Ch13. (19) *Gnathodus pseudosemiglaber* Thompson and Fellows, 1970; Upper view of IUMC 780, sample Ch29. (20) *Gnathodus semiglaber* Bischoff, 1957; Upper view of IUMC 781, sample Ch26. (21) *Protognathodus meischneri* Ziegler, 1969; Upper view of IUMC 782, sample Ch24. (22) *Gnathodus pseudosemiglaber* Thompson and Fellows, 1970; Upper view of IUMC 783, sample Ch28. (23) *Protognathodus collinsoni* Ziegler, 1969; Upper view of IUMC 784, sample Ch22. (24) *Protognathodus collinsoni* Ziegler, 1969; Upper view of IUMC 785, sample Ch24. (25) *Protognathodus collinsoni* Ziegler, 1969; Upper view of IUMC 786, sample Ch22. (26) *Branmehla inornata* (Branson and Mehl, 1934); Upper view of IUMC 787, sample Ch13. (27) *Gnathodus semiglaber* Bischoff, 1957; Upper view of IUMC 788, sample Ch27. (28) *Gnathodus cuneiformis* Mehl and Thomas, 1947; Upper view of IUMC 789, sample Ch27. (29) *Polygnathus communis communis* (Branson and Mehl, 1934); Upper view of IUMC 790 (a juvenile form), sample Ch7. (30) *Palmatolepis gracilis expansa* Sandberg and Ziegler, 1979 Morphotyp 1; Upper view of IUMC 791, sample Ch12. (31) *Polygnathus nodocostatus nodocostatus* Branson and Mehl, 1934; Upper view of IUMC 792, sample Ch11. (32) *Bispathodus bispathodus* Ziegler et al., 1974; Upper view of IUMC 793, sample Ch15. (33) *Polygnathus communis communis* (Branson and Mehl, 1934); Upper view of IUMC 794, sample Ch15. (34) *Palmatolepis minuta minuta* Branson and Mehl, 1934; Upper view of IUMC 795, sample Ch7. (35) *Bispathodus jugosus* (Branson and Mehl, 1934); Upper view of IUMC 796, sample Ch13. (36) ?*Siphonodella praesulcata* Sandberg et al., 1972; Lower view of IUMC 797, sample Ch16-1. (37) *Bispathodus costatus* (Branson, 1934) Morphotyp 2; Upper view of IUMC 798, sample Ch15. (38) *Bispathodus jugosus* (Branson and Mehl, 1934); Upper view of IUMC 799, sample Ch12. (39) *Polygnathus padovanii* Perri and Spalletta, 1990; Upper view of IUMC 800, sample Ch6. (40) *Pandorinellina insita* Müller, 1956; Upper view of IUMC 801, sample Ch10

(sample numbers: EUIC), University of Isfahan, I.R. Iran. Repository numbers of the figured specimens are given in the explanations of plates (Figs. 5, 6, 7 and 8).

Conodont distribution

338 conodont elements from the Chelcheli section around the DCB lead to the discrimination of 15 biostratigraphical intervals (Fig. 4; Table 1) and to the identification of 47 species and subspecies within fifteen genera: *Alternognathus*, *Bispathodus*, *Branmehla*, *Clydagnathus*, *Gnathodus*, *Icriodus*, *Mehlina*, *Palmatolepis*, *Polygnathus*, *Protognathodus*, *Pseudopolygnathus*, *Scaliognathus, Doliognathus, Siphonodella* and *Scaphignathus* utilized to establish the biostratigraphical framework for the studied section (Table 1). Overall, the preservation of the conodont elements is good, but a number of broken elements also collected were not identified. The Color Alteration Index (CAI) of conodonts (Epstein et al. 1977) is 4–4.5. In this report we use the revised conodont zonation published by Spalletta et al. (2017) until the first occurrence of *Siphonodella praesulcata*, then we continue to apply the conodont zonation published in Kaiser et al. (2009) which means *praesulcata* Zone (= old Lower *praesulcata* Zone), *ck*I (extinction-based *costatus-kockeli* Interregnum), *kockeli* Zone (= old Upper *praesulcata* Zone), and *sulcata/kuehni* Zone (= old *sulcata* Zone). This was done for two reasons, first Spalletta et al. (2017) substituted the *praesulcata* Zone, and their *ultimus* Zone includes the *praesulcata* Zone and the *ck*I, and second, we have not found biostratigraphically significant *Protognathodus* species (such as *Protognathodus kockeli* or *Protognathodus kuehni*) in this section. The occurring *Protognathodus* fauna is mainly represented by *Protognathodus meischneri* and *Protognathodus collinsoni*.

The conodont zonation for the Mississippian utilized was proposed by Sandberg et al. (1978), Kaiser et al. (2009) and Becker et al. (2016). The zonation, proposed as preliminary standard conodont zonation by Lane et al. (1980), was applied for the biostratigraphic analysis of the upper Tournaisian conodont zonation. The Tournaisian conodont biozones nearly always indicated by the markers, some species of the genera *Gnathodus*, *Pseudoplygnathus*, *Scaliognathus*, *Doliognathus* and *Siphonodella* were utilized in recognizing the biozones.

The basal part of the section (sample Ch1) yielded only a few icriodid specimens (*Icriodus alternatus alternatus, Icriodus alternatus helmsi* and *Icriodus cornutus*). Due to the lack of index conodont fauna, the precise position of this succession cannot be determined (Table 1).

***Palmatolepis minuta minuta* Zone** (sample Ch2)

The lower limit of this zone is recognized by the entry of *Palmatolepis minuta minuta* Branson and Mehl, 1934, ranging from the *Palmatolepis minuta minuta* Zone to the *Pseudopolygnathus granulosus* Zone (Spalletta et al. 2017) which corresponds to the former Upper *triangularis*—Upper

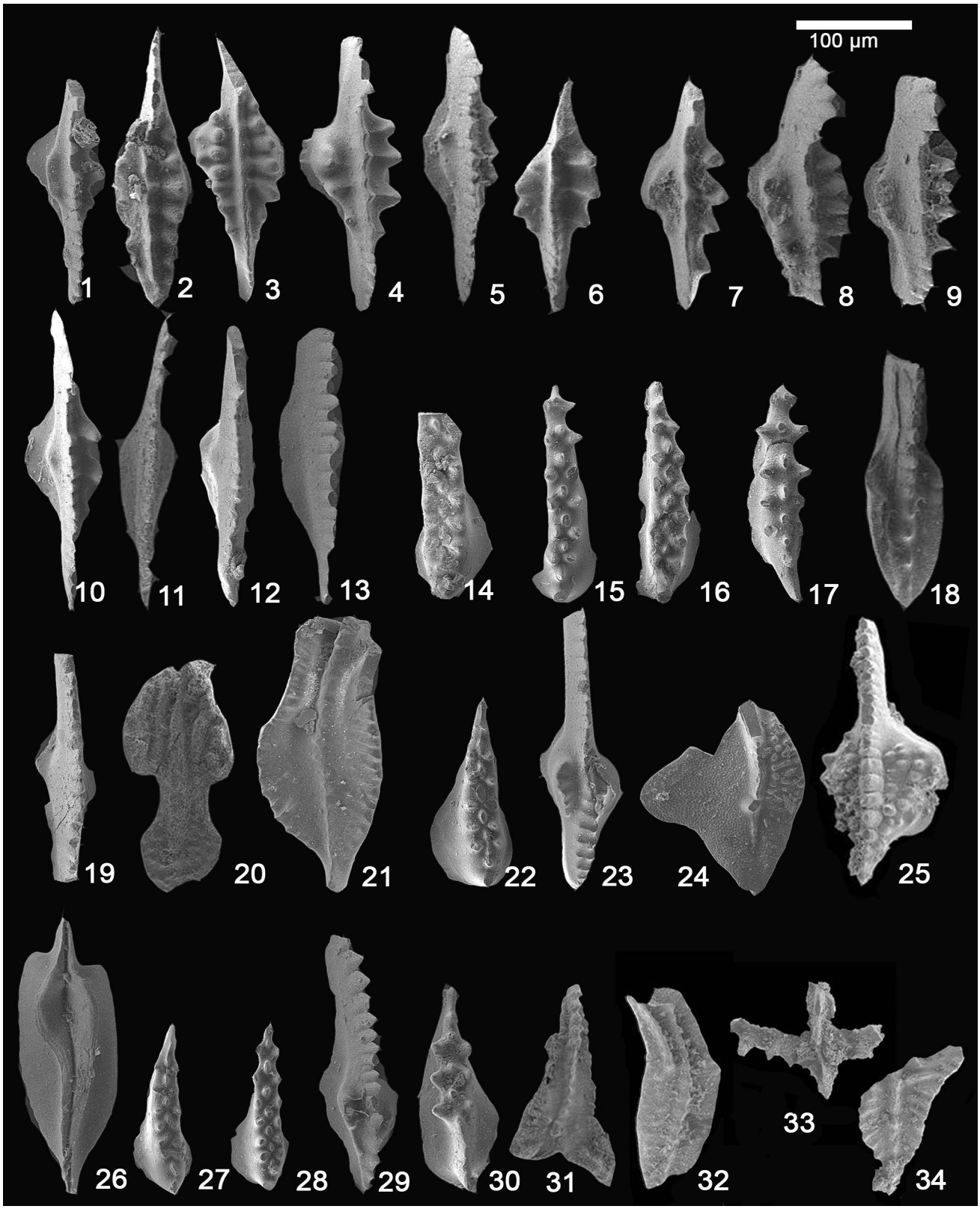
100 µm
1
2
3
4
5
6
7
8
9
10
11
12
13
14
15
16
17
18
19
20
21
22
23
24
25
26
27
28
29
30
31
32
33
34

◂**Fig. 7** Conodonts from the Chelcheli section, the scale bar is 100 µm. (1) *Bispathodus aculeatus aculeatus* (Branson and Mehl, 1934); upper view of IUMC 804, sample Ch5. (2) *Alternognathus regularis regularis* Ziegler and Sandberg, 1984; upper view of IUMC 805, sample Ch9. (3) *Pseudopolygnathus primus* M2 Branson and Mehl, 1934; Upper view of IUMC 806, sample Ch21. (4) *Pseudopolygnathus primus* M2 Branson and Mehl, 1934; upper view of IUMC 807, sample Ch22. (5) *Bispathodus aculeatus aculeatus* (Branson and Mehl, 1934); Upper view of IUMC 808, sample Ch14. (6) *Pseudopolygnathus primus* M2 Branson and Mehl, 1934; Upper view of IUMC 809, sample Ch22. (7) *Bispathodus aculeatus aculeatus* (Branson and Mehl, 1934); upper view of IUMC 810, sample Ch14. (8) *Pseudopolygnathus primus* M2 Branson and Mehl, 1934; Upper view of IUMC 811, sample Ch21. (9) *Pseudopolygnathus primus* M2 Branson and Mehl, 1934; Upper view of IUMC 812, sample Ch22. (10) *Bispathodus aculeatus aculeatus* (Branson and Mehl, 1934); upper view of IUMC 815, sample Ch13. (11) *Bispathodus stabilis vulgaris* (Dzik, 2006); upper view of IUMC 816, sample Ch10. (12) *Bispathodus stabilis vulgaris* (Dzik, 2006); upper view of IUMC 817, sample Ch13, X 150. (13) *Bispathodus stabilis stabilis* (Branson and Mehl, 1934); upper view of IUMC 818, sample Ch13. (14) *Icriodus alternatus helmsi* Sandberg and Dreesen, 1984; upper view of IUMC 820, sample Ch3. (15) *Icriodus alternatus helmsi* Sandberg and Dreesen, 1984; upper view of IUMC 821, sample Ch3. (16) *Icriodus alternatus helmsi* Sandberg and Dreesen, 1984; upper view of IUMC 822, sample Ch3. (17) *Icriodus cornutus* Sannemann, 1955a; upper view of IUMC 823, sample Ch4. (18) *Polygnathus communis dentatus* (Druce, 1969); upper view of IUMC 824, sample Ch14. (19) *Bispathodus stabilis vulgaris* (Dzik, 2006); upper view of IUMC 825, sample Ch14. (20) *Polygnathus triphyllatus* Helms, 1961; upper view of IUMC 826, sample Ch7. (21) *Polygnathus inornatus* Branson, 1934; upper view of IUMC 827, sample Ch26. (22) *Icriodus alternatus alternatus* Branson and Mehl, 1934 Morphotyp 1; upper view of IUMC 828, sample Ch2. (23) *Gnathodus pseudosemiglaber* Thompson and Fellows, 1970; upper view of IUMC 829, sample Ch30. (24) *Palmatolepis quadrantinodosalobata* Sannemann, 1955a; upper view of IUMC 830, sample Ch4. (25) *Gnathodus* cf. *punctatus* (Cooper, 1939); upper view of IUMC 831, sample Ch26. (26) *Polygnathus inornatus* Branson, 1934; lower view of IUMC 832, sample Ch26. (27) *Icriodus alternatus helmsi* Sandberg and Dreesen, 1984; upper view of IUMC 833, sample Ch2. (28) *Icriodus alternatus helmsi* Sandberg and Dreesen, 1984; upper view of IUMC 834, sample Ch2. (29) *Protognathodus meischneri* Ziegler, 1969; upper view of IUMC 835, sample Ch18. (30) *Icriodus alternatus alternatus* Branson and Mehl, 1934 Morphotyp 1; Upper view of IUMC 836, sample Ch4. (31) *Doliognathus latus* Branson and Mehl, 1941 Morphotype 2; upper view of IUMC 836, sample Ch4. (32) *Siphonodella obsoleta* Hass, 1959; upper oblique view of IUMC 836, sample Ch4. (33) *Scaliognathus anchoralis europensis* Lane and Ziegler, 1983; upper oblique view of IUMC 836, sample Ch4. (34) *Pseudopolygnathus* cf. *pinnatus* Voges, 1959 Morphotype 1; upper oblique view of IUMC 836, sample Ch4

trachytera zones (Ji and Ziegler 1993) of Ziegler and Sandberg (1990). *Icriodus alternatus alternatus, Icriodus alternatus helmsi* and *Icriodus cornutus* are the accompanying conodont species.

***Palmatolepis crepida* Zone** (sample Ch3)

Polygnathus nodocostatus nodocostatus Branson and Mehl, 1934 was found in sample Ch3. This species ranges from the *Palmatolepis crepida* Zone to the *Palmatolepis gracilis expansa* Zone (Spalletta et al. 2017) and was found in various samples from Ch3 up to Ch11. *Polygnathus communis communis, Icriodus alternatus alternatus, Icriodus alternatus helmsi* and *Icriodus cornutus* are additional conodont species in this sample.

***Palmatolepis termini* Zone** to ***Palmatolepis glabra prima* Zone** (sample Ch4)

The entry of *Polygnathus semicostatus* Branson and Mehl, 1934 in sample Ch4 lead to the attribution of this sample to the *Palmatolepis termini* Zone. This species first appears in the lower *Palmatolepis termini* Zone (Ji and Ziegler 1993; Spalletta et al. 2017). *Palmatolepis minuta minuta, Icriodus alternatus alternatus* and *Icriodus cornutus* are the other associated species. There are no condodonts diagnostic for the *Palmatolepis glabra prima* Zone.

***Palmatolepis glabra pectinata* Zone** to ***Palmatolepis rhomboidea* zones interval** (sample Ch4-1)

Sample Ch4-1 yielded *Palmatolepis quadrantinodosalobata* Sannemann, 1955a M1 Sandberg and Ziegler, 1973 and *Polygnathus padovanii* Perri and Spalletta, 1990, both have their first occurrence within the *Palmatolepis glabra pectinata* Zone (Spalletta et al. 2017). No other conodonts were found in this interval.

***Palmatolepis gracilis gracilis* Zone** to ***Palmatolepis marginifera utahensis* Zone** (samples Ch5–Ch6)

The index conodont species *Palmatolepis gracilis gracilis* Branson and Mehl, 1934 ranges from the Upper *rhomboidea* Zone (Klapper and Ziegler 1980; Ji and Ziegler 1993), the *Palmatolepis gracilis gracilis* Zone of Spalletta et al. (2017). The presence of *Palmatolepis gracilis gracilis* in sample Ch5 allows the attribution of the level of this sample to the *Palmatolepis gracilis gracilis* Zone. *Polygnathus triphyllatus* Helms, 1961 which range starts within the basal part of the *Palmatolepis gracilis gracilis* Zone is also present in sample Ch5. The upper limit of the interval was defined by the entry of *Scaphignathus velifer velifer* in sample Ch7. *Polygnathus padovanii*, *Polygnathus semicostatus, Polygnathus nodocostatus nodocostatus, Polygnathus communis communis, Palmatolepis minuta minuta,* and *Icriodus cornutus* are the associated species in this interval.

***Scaphignathus velifer velifer* Zone** (sample Ch7)

The entry of the index species *Scaphignathus velifer velifer* Helms, 1959 is the marker for the lower limit of this zone, the conodont species *Alternognathus regularis regularis* Ziegler and Sandberg, 1984 also has its first occurrence at

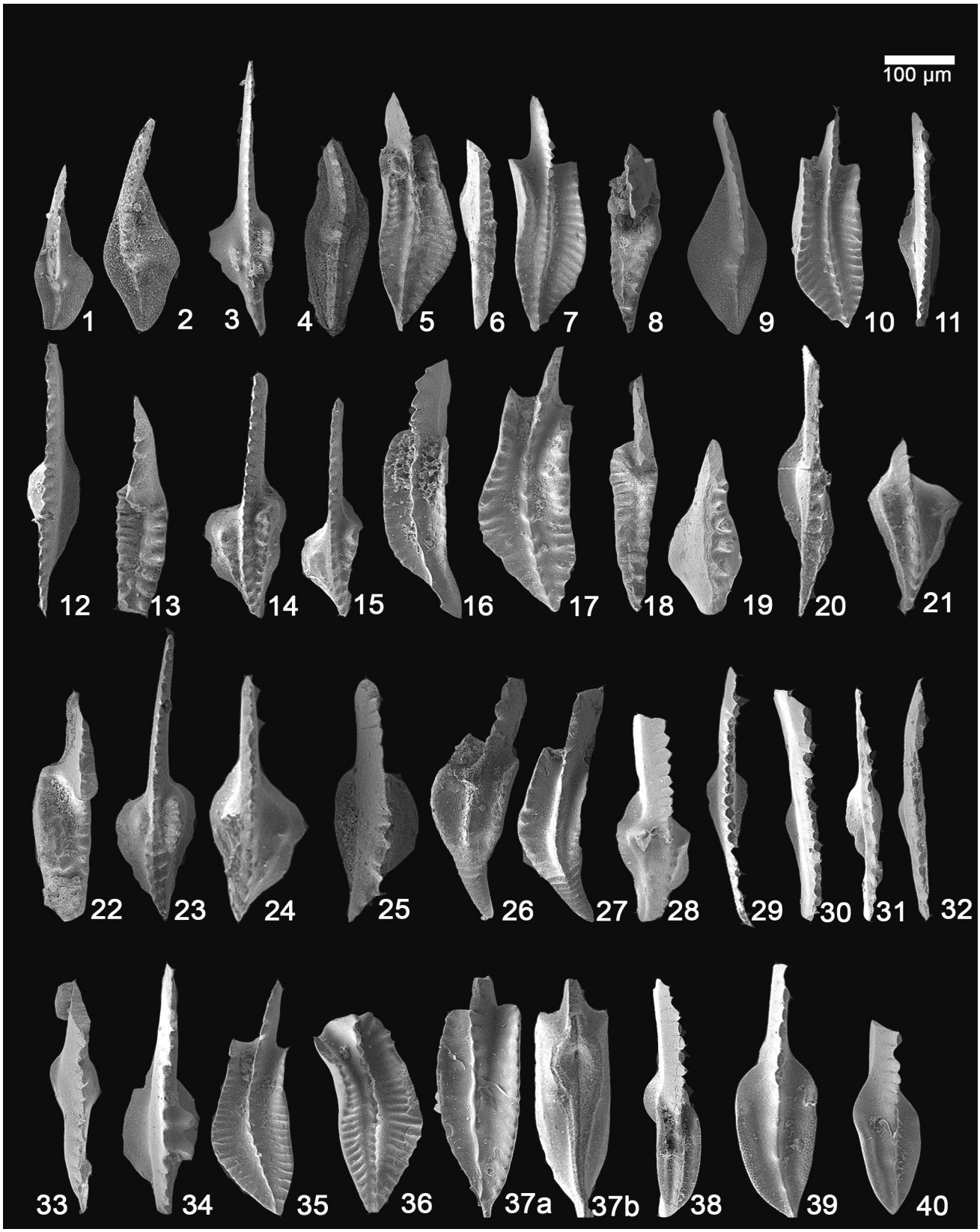
100 µm
1
2
3
4
5
6
7
8
9
10
11
12
13
14
15
16
17
18
19
20
21
22
23
24
25
26
27
28
29
30
31
32
33
34
35
36
37a
37b
38
39
40

◂**Fig. 8** Conodonts from the Chelcheli section, the scale bar is 100 µm. (1) *Palmatolepis minuta minuta* Branson and Mehl, 1934; upper view of IUMC 838, sample Ch6. (2) *Palmatolepis minuta minuta* Branson and Mehl, 1934; upper view of IUMC 839, sample Ch6. (3) *Gnathodus pseudosemiglaber* Thompson and Fellows, 1970; Upper view of IUMC 840, sample Ch35. (4) *Palmatolepis gracilis gonioclymeniae* Müller, 1956; upper view of IUMC 841, sample Ch16-1. (5) *Polygnathus inornatus* Branson, 1934; upper view of IUMC 842, sample Ch21. (6) *Bispathodus costatus* (Branson, 1934) Morphotyp 2; upper view of IUMC 843, sample Ch16-1. (7) *Polygnathus inornatus* Branson, 1934; upper view of IUMC 844, sample Ch24. (8) *Clydagnathus cavusformis* Rhodes et al., 1969; upper view of IUMC 845, sample Ch20. (9) *Palmatolepis minuta minuta* Branson and Mehl, 1934; upper view of IUMC 846, sample Ch9. (10) *Polygnathus inornatus* Branson, 1934; upper view of IUMC 847, sample Ch24. (11) *Bispathodus stabilis stabilis* (Branson and Mehl, 1934); upper view of IUMC 848, sample Ch24. (12) *Bispathodus stabilis vulgaris* (Dzik, 2006); upper view of IUMC 849, sample Ch18. (13) *Clydagnathus cavusformis* Rhodes et al., 1969; upper view of IUMC 850, sample Ch18. (14) *Gnathodus cuneiformis* Mehl and Thomas, 1947; upper view of IUMC 851, sample Ch27. (15) *Gnathodus cuneiformis* Mehl and Thomas, 1947; upper view of IUMC 852, sample Ch27. (16) *Polygnathus longiposticus* Branson and Mehl, 1934; upper view of IUMC 853, sample Ch26. (17) *Polygnathus inornatus* Branson, 1934; upper view of IUMC 854, sample Ch26. (18) *Scaphignathus velifer velifer* Helms, 1959; upper view of IUMC 855, sample Ch9. (19) *Bispathodus aculeatus* ssp. upper view of IUMC 856, sample Ch15. (20) *Bispathodus costatus* (Branson, 1934) Morphotyp 1; upper view of IUMC 857, sample Ch15. (21) *Protognathodus meischneri* Ziegler, 1969; upper view of IUMC 858, sample Ch18, X 150. (22) *Scaphignathus velifer velifer* Helms, 1959; upper view of IUMC 859, sample Ch8. (23) *Gnathodus pseudosemiglaber* Thompson and Fellows, 1970; Upper view of IUMC 860, sample Ch28. (24) *Protognathodus meischneri* Ziegler, 1969; upper view of IUMC 861, sample Ch21. (25) *Protognathodus meischneri* Ziegler, 1969; upper view of IUMC 862, sample Ch21. (26) *Polygnathus semicostatus* Branson and Mehl, 1934; upper view of IUMC 863, sample Ch12. (27) *Polygnathus semicostatus* Branson and Mehl, 1934; upper view of IUMC 864, sample Ch12. (28) *Protognathodus meischneri* Ziegler, 1969; upper view of IUMC 865, sample Ch22. (29) *Branmehla inornata* (Branson and Mehl, 1934); upper view of IUMC 866, sample Ch16. (30) *Mehlina strigosa* (Branson and Mehl, 1934); upper view of IUMC 867, sample Ch15. (31) *Branmehla ampla* (Branson and Mehl, 1934); upper view of IUMC 868, sample Ch13. (32) *Pandorinellina insita* Müller, 1956; upper view of IUMC 869, sample Ch10. (33) *Branmehla bohlenana bohlenana* (Helms, 1959); upper view of IUMC 870, sample Ch10. (34) *Bispathodus aculeatus aculeatus* (Branson and Mehl, 1934); upper view of IUMC 871, sample Ch13. (35) *Polygnathus inornatus* Branson, 1934; Upper view of IUMC 872, sample Ch21. (36) *Polygnathus inornatus* Branson, 1934; Upper view of IUMC 873, sample Ch21. (37) *Polygnathus longiposticus* Branson and Mehl, 1934; upper (a) and lower (b) views of IUMC 874, sample Ch21. (38) *Polygnathus communis communis* (Branson and Mehl, 1934); upper view of IUMC 875, sample Ch9. (39) *Polygnathus communis communis* (Branson and Mehl, 1934); upper view of IUMC 876, sample Ch11. (40) *Polygnathus communis communis* (Branson and Mehl, 1934); upper view of IUMC 877, sample Ch10

the base of the *Scaphignathus velifer velifer* Zone (Spalletta et al. 2017). *Palmatolepis minuta minuta, Palmatolepis gracilis gracilis, Polygnathus padovanii, Branmehla bohlenana bohlenana, Polygnathus semicostatus, Polygnathus communis communis, Polygnathus nodocostatus nodocostatus* and *Icriodus cornutus* are present in this sample, too.

***Palmatolepis rugosa trachytera* Zone** (sample Ch8)

The entry of zonal index species *Palmatolepis rugosa trachytera* Ziegler, 1960 in sample Ch8 is the marker of the lower limit of the zone (Ji and Ziegler 1993; Spalletta et al. 2017). *Scaphignathus velifer velifer, Palmatolepis minuta minuta, Palmatolepis gracilis gracilis, Polygnathus padovanii, Alternognathus regularis regularis, Branmehla bohlenana bohlenana, Polygnathus semicostatus, Polygnathus communis communis, Polygnathus nodocostatus nodocostatus,* and *Icriodus cornutus* are the other species found in this sample.

***Pseudopolygnathus granulosus* Zone** to ***Palmatolepis gracilis manca* Zone** (samples Ch9–Ch10)

The base of this interval can be recognized by the entry of *Palmatolepis gracilis sigmoidalis* Ziegler, 1962. The last occurrence of *Palmatolepis minuta minuta* Branson and Mehl, 1934 and *Icriodus cornutus* Sannemann, 1955b was utilized to identifying the *Pseudopolygnathus granulosus* Zone. Spalletta et al. (2017) considered *Palmatolepis gracilis sigmoidalis* as a useful taxon for the identification of the *Pseudopolygnathus granulosus* Zone. *Polygnathus granulosus, Bispathodus stabilis vulgaris, Branmehla ampla, Branmehla inornata* can be observed at the top of this interval. The indicative species of the *Polygnathus styriacus* and *Palmatolepis gracilis manca* zones are missing. *Scaphignathus velifer velifer, Palmatolepis gracilis gracilis, Polygnathus padovanii, Branmehla bohlenana bohlenana, Polygnathus semicostatus, Polygnathus communis communis, Polygnathus nodocostatus nodocostatus, Mehlina strigosa* and *Alternognathus regularis regularis* are also present in these samples.

***Palmatolepis gracilis expansa* Zone** (sample Ch11)

The entry of zonal index species *Palmatolepis gracilis expansa* Sandberg and Ziegler, 1979 in Ch11 defines the base of this zone. *Bispathodus jugosus* (Branson and Mehl, 1934) is also a good marker for this zone (Ziegler and Sandberg 1984; Ji and Ziegler 1993; Spalletta et al. 2017). *Bispathodus bispathodus, Bispathodus stabilis stabilis, Branmehla inornata, Bispathodus stabilis vulgaris, Polygnathus granulosus, Branmehla ampla, Palmatolepis gracilis sigmoidalis, Mehlina strigosa,* and *Alternognathus regularis regularis* are some associated species. *Alternognathus regularis regularis* ends at the top of the *Palmatolepis gracilis manca* Zone (Spalletta et al. 2017), but at the Chelcheli section it is possible to extend the range.

Table 1 Distribution chart of conodont species in the Chelcheli section

Chelcheli section	ch1	ch2	ch3	ch4	ch4-1	ch5	ch6	ch7	ch8	ch9	ch9-1	ch10	ch11	ch12	ch13	ch14	ch15	ch16-1	ch17	ch18	ch19	ch20	ch21	ch22	ch23	ch24	ch25	ch26	ch26-1	ch27	ch28	ch29	ch30	ch31	ch32	ch33	Total
Alternognathus regularis regularis								1	1	1		1	1																								5
Bispathodus aculeatus aculeatus															5	2	3	2																			12
Bispathodus bispathodus													1	2	1	2	1	2																			9
Bispathodus costatus M1															2	1	2	1																			6
Bispathodus costatus M2															1	1	3	1																			6
Bispathodus jugosus													1	1	2	1	1																				6
Bispathodus spinulicostatus															1			2		1																	4
Bispathodus stabilis stabilis													1		1	2	2	1		1						1											9
Bispathodus stabilis vulgaris												1	1		1	1	2	1		1	1	3															12
Branmehla ampla												1	1		1																						3
Branmehla bohlenana bohlenana								1	1	2		1	2																									7
Branmehla inornata												1	1		1	2	1	1		1	2	1	2	1													14
Clydagnathus plumulus														1	2	3	3	2																			11
Clydagnathus cavusformis																				1	2	1															4
Doliognathus latus M2																														1							1
Gnathodus cuneiformis																												1	1	1	1						4
Gnathodus punctatus																												1	1								2
Gnathodus pseudosemiglaber																														1	2	3	1	1	2	1	11
Gnathodus semiglaber																												1	1	2	1	1	2				8

Table 1 (continued)

Chelcheli section	ch1	ch2	ch3	ch4	ch4-1	ch5	ch6	ch7	ch8	ch9	ch9-1	ch10	ch11	ch12	ch13	ch14	ch15	ch16-1	ch17	ch18	ch19	ch20	ch21	ch22	ch23	ch24	ch25	ch26	ch26-1	ch27	ch28	ch29	ch30	ch31	ch32	ch33	Total
Icriodus alternatus alternatus	1	2	5	11																																	19
Icriodus alternatus helmsi	1	1	1																																		3
Icriodus cornutus	1	1	1	3		1	1	1	2	1																											12
Mehlina strigosa											1	1	1	1	1	1	1	1																			8
Polygnathus communis communis			2			1	2	2	1	1	2	1	2	2	3	1		1																			21
Palmatolepis gracilis expansa													1	1	2	1	1	1																			7
Palmatolepis gracilis goniocylmenia																		1																			1
Palmatolepis gracilis gracilis						1	1	1	1	1		1	1	1	1	1																					10
Palmatolepis gracilis sigmoidalis											1		1	2	1	1	2	1																			9
Palmatolepis minuta minuta		1	1	3		1	1	1	1	1	2	1																									13
Palmatolepis quadrantinodosalobata					1																																1
Palmatolepis rugosa trachytera									1																												1
Polygnathus granulosus												1	1	1	2	1	1																				7
Polygnathus inornatus																	1	3		2			2	1	1	2	1	1									14
Polygnathus longiposticus																			1	1			2	1	2	1	1	1									10
Polygnathus nodocostatus nodocostatus			1			1	1	1	1	1		1	1																									8

Table 1 (continued)

Chelcheli section	ch1	ch2	ch3	ch4	ch4-1	ch5	ch6	ch7	ch8	ch9	ch9-1	ch10	ch11	ch12	ch13	ch14	ch15	ch16-1	ch17	ch18	ch19	ch20	ch21	ch22	ch23	ch24	ch25	ch26	ch26-1	ch27	ch28	ch29	ch30	ch31	ch32	ch33	Total
Polygnathus padovanii					1	1	1	1	1																													5
Polygnathus semicostatus			1			1	2	2	4	1		1	2	1	3	1	3																					22
Polygnathus triphyllatus								1	1	1																												3
Protognathodus collinsoni																1	1		1					2		2												7
Protognathodus meischneri																1	1	1	1	1			1	1	1	1												9
Pseudopolygnathus primus M2																		2		2			1	1	1	1												8
Pseudopolygnathus cf. pinnatus																														1								1
Scaphignathus velifer velifer								1	1	1	1																											4
Scaliognathus anchoralis europensis																														1								1
Siphonodella obsoleta																										1												1
Siphonodella praesulcata																		1																				1
Total	3	5	12	17	2	7	9	13	16	11	7	12	19	13	31	24	29	25	3	11	5	5	8	7	5	9	2	5	3	7	4	4	3	1	2	1	340

***Bispathodus aculeatus aculeatus* Zone** (sample Ch12)

This zone corresponds to the lower part of the former Middle *expansa* Zone and is equivalent to the lower subzone of the *Bispathodus aculeatus aculeatus* Zone of Hartenfels (2011). The lower limit can be defined by the first occurrence of zonal index species *Bispathodus aculeatus aculeatus* (Branson and Mehl, 1934). This species extends into the Visean (*texanus* Zone; Lane et al. 1980; Spalletta et al. 2017). *Palmatolepis gracilis expansa, Bispathodus bispathodus, Bispathodus jugosus, Polygnathus granulosus, Palmatolepis gracilis sigmoidalis, Palmatolepis gracilis gracilis, Polygnathus semicostatus* and *Polygnathus communis communis* are the associated species.

***Bispathodus costatus* Zone** (sample Ch13)

This new proposed zone (Spalletta et al. 2017) is equivalent to the upper part of the Middle *expansa* Zone, and to the Lower *costatus* Zone of Ziegler (1962). It is the same as proposed by Corradini et al. (2016) and corresponds to the *Bispathodus costatus* Subzone of Hartenfels (2011). The first entry of marker species *Bispathodus costatus* (Branson, 1934) M1 and *Bispathodus costatus* (Branson, 1934) M2 defines the lower limit of this zone. In addition, *Bispathodus spinulicostatus, Clydagnathus plumulus, Bispathodus aculeatus aculeatus, Bispathodus stabilis stabilis, Bispathodus jugosus, Palmatolepis gracilis sigmoidalis, Palmatolepis gracilis gracilis, Polygnathus semicostatus* and *Polygnathus communis communis* and some other species were found in this sample.

***Bispathodus ultimus* Zone** (Ch14–Ch16 and Ch16-1)

This relatively large new defined *ultimus* Zone (Spalletta et al. 2017) is equivalent to the Upper *expansa*, Lower and Middle *praesulcata* zones of Ziegler and Sandberg (1984), as well as to the Upper *expansa* and *praesulcata* zones and the *costatus–kockeli* Interregnum of Kaiser et al. (2009); (see comments at the beginning of "Conodont distribution"). Although the base of the *costatus-kockeli* Interregnum (*ck*I) is linked with a global and sudden extinction of a number of conodonts, such as the *Bi. costatus—ultimus* Group, among others, the collected samples did not yield the index conodont species *Bispathodus ultimus,* the association with *Protognathodus meischneri* Ziegler, 1969, *Protognathodus collinsoni* Ziegler, 1969, *Palmatolepis gracilis gonioclymeniae* Müller, 1956 and *Siphonodella praesulcata* Sandberg et al., 1978, most likely suggests the *Bispathodus ultimus* Zone. Lithologically, the *Bispathodus ultimus* Zone corresponds to rocks of the upper part of unit 3 and unit 4 of the succession, in which shale, marl and limestone gradually change to very tiny alternation of platy black shales with intercalated sandstones (Fig. 3d). This succession is overlain by thick-bedded quartzitic sandstone. This characteristic lithology represents most likely equivalents of both, the Hangenberg Black Shale (HBS) and the Hangenberg Sandstone (HSS).

?***Protognathodus kockeli* Zone** to **L. *Siphonodella crenulata* Zone** (sample Ch17–Ch25)

Although the zonal marker species *Protognathodus kockeli, Protognathodus kuehni* and *Siphonodella sulcata* were not found in the collected samples, the association of *Polygnathus inornatus, Polygnathus longiposticus, Clydagnathus cavusformis, Pseudopolygnathus primus* M2, *Protognathodus meischneri, Protognathodus collinsoni* and the entry of *Siphonodella obsoleta* in the level of sample Ch24 lead to the attribution of this interval to the latest Famennian/Early Mississippian ?*Pr. kockeli* to L. *Si. crenulata* zones. *Pr. meischneri* and *Pr. collinsoni* are atypical forms, as they do not correspond in detail to the original diagnosis. The sedimentological changes from the white quartzitic sandstone (HSS) to the micritic limestone at the base of sample Ch17 is considered as the DCB, thus, more research on that specific point is necessary.

***Siphonodella isosticha*—U. *Siphonodella crenulata* Zone** and ***Gnathodus typicus* Zone** (samples Ch26–Ch26-1)

The lower limit of this interval is well defined by the first entry of *Gnathodus semiglaber* Bischoff, 1957, *Gnathodus cuneiformis* Mehl and Thomas, 1947 and *Gnathodus punctatus* Cooper, 1939 in sample Ch26. All species have their first occurrences at the base of the *isosticha* to Upper *crenulata* Zone and range into the Lower *typicus* Zone (Lane et al. 1980) and/or into the *anchoralis—latus* Zone (Voges 1959) or even higher into the Visean.

***Scaliognathus anchoralis—Doliognathus latus* Zone** (samples Ch27–Ch35)

This zone is characterized in the upper part of the studied section by the entry of the zonal marker species *Scaliognathus anchoralis europensis* Lane and Ziegler, 1983 and *Doliognathus latus* Branson and Mehl, 1941 Morphotype 2 in sample Ch27. *Gnathodus pseudosemiglaber* Thompson and Fellows, 1970 and *Pseudopolygnathus* cf. *pinnatus* Voges, 1959 also have their first occurrences at the base of this zone (Lane et al. 1980).

Conclusion

Late Palaeozoic Upper Devonian to Mississippian rocks in shallow-water facies were studied in the Chelcheli section. The major finding can be summarized as follows:

- The more or less complete section ranges from the *Palmatolepis minuta minuta* into the *Scaliognathus anchoralis-Doliognathus latus* Zone.
- Due to the overall shallow-water palaeoenvironment the conodont record is not excellent but most conodont zones from the Late Devonian to the Mississippian can be distinguished.
- Close to the DCB there is a small hiatus which might be a result of facies (shallow-water succession with no conodont record and siliciclastic rocks) rather than the period of non-deposition as the sedimentological record seems continuous.
- In contrast to other DCB sections described from Iran (Königshof et al. 2021), the Chelcheli section exhibits a characteristic lithology around the DCB known from many other places around the world.
- The black shales and the superimposed thick-bedded quartzitic sandstones represent equivalents of the Hangenberg Black Shale (HBS) and the Hangenberg Sandstone (HSS), respectively.
- The conodont association around the DCB provides important information in the frame of the recent discussion on a revision of this boundary.

Acknowledgements Iliana Boncheva, Claudia Spalletta, Mehdi Yazdi, and the Editor-in-Chief Mike Reich are thanked for constructive reviews of the submitted manuscript. The authors are grateful to Office of Vice Chancellor for Research and Technology at the University of Isfahan for financial and technical support. This study was undertaken at the University of Isfahan in cooperation with the Senckenberg Research Institute and Natural History Museum, Frankfurt. This is a contribution to the International Geoscience Programme IGCP 652 and IGCP 700. One of the authors (P.K.) acknowledges funding by the Deutsche Forschungsgemeinschaft (DFG; KO 1622/16-1).

References

Abadi, M.S., A.C. Da Silva, H. Mossadegh, S. Spassov, and F. Boulvain. 2015. Lower Carboniferous ramp sedimentation of the Central Alborz Basin, northern Iran: integrated sedimentological and rock-magnetic studies. In *Magnetic susceptibility application: a window onto ancient environments and climate variations*, eds. A.C. Da Silva, M.T. Whalen, J. Hladil, L. Chadimova, D. Chen, S. Spassov, F. Boulvain, and X. Devleeschouwer. *Geological Society of London, Special Publications* 414: 73–91.

Ahmadzadeh-Heravi, H.M. 1975. Stratigraphie und Fauna im Devon des östlichen Elburs Iran. *Clausthaler Geologische Abhandlungen* 23: 1–114.

Alavi, M. 1991. Sedimentary and structural characteristics of the Paleo-Tethys remnants in northeastern Iran. *Geological Society of America, Bulletin* 103: 983–992.

Alavi, M. 1996. Tectonostratigraphic synthesis and structural style of the Alborz mountain system in northern Iran. *Journal of Geodynamics* 21: 1–33.

Aretz, M., C. Corradini, and J. Denayer. 2021. The Devonian-Carboniferous Boundary around the globe: a complement. *Palaeobiodiversity and Palaeoenvironments* 101: 633–662.

Ashouri, A.R. 1994. The stratigraphical position of members 1 and 6 of Khoshyeilagh Formation based on conodont fauna and introduction of three conodont zones from member 6. *Geo Sciences Scientific Quarterly Journal* 13: 64–71. (in Persian).

Ashouri, A.R. 2006. Middle Devonian-Early Carboniferous conodont faunas from the Khoshyeilagh Formation, Alborz Mountains, North Iran. *Journal of Sciences, Islamic Republic of Iran* 17: 53–65.

Ashouri, A.R. 1990. *Devonian and Carboniferous conodont faunas from Iran,* 1–351. Unpublished PhD thesis, University of Hull.

Bábek, O., T. Kumpan, J. Kalvoda, and T.M. Grygar. 2016. Devonian/Carboniferous boundary glacioeustatic fluctuations in a platform-to-basin direction: a geochemical approach of sequence stratigraphy in pelagic settings. *Sedimentary Geology* 337: 81–99.

Bagheri, S., and G.M. Stampfli. 2008. The Anarak, Jandaq and Posht-e-Badam metamorphic complexes in central Iran: new geological data, relationships and tectonic implications. *Tectonophysics* 451: 123–155.

Bahrami, A., C. Corradini, D.J. Over, and M. Yazdi. 2011. Upper Devonian-Lower Carboniferous conodont biostratigraphy in the Shotori Range, Tabas area, Central-East Iran Microplate. *Bollettino della Società Paleontologica Italiana* 50: 35–53.

Bahrami, A., P. Königshof, I. Boncheva, M. Yazdi, M. Ahmadi Nahre Khalaji, and E. Zarei. 2018. Conodont biostratigraphy of the Kesheh and Dizlu sections, and the age range of the Bahram Formation in Central Iran. *Palaeobiodiversity and Palaeoenvironments* 98: 315–329.

Bahrami, A., P. Königshof, H. Vaziri-Moghaddam, B. Shakeri, and I. Boncheva. 2019. Conodont stratigraphy and conodont biofacies of the shallow-water Kuh-e-Bande-Abdol-Hossein section (SE Anarak, Central Iran). *Palaeobiodiversity and Palaeoenvironments* 99: 477–494.

Becker, R.T., S.I. Kaiser, and M. Aretz. 2016. Review of chrono- litho- and biostratigraphy across the global Hangenberg Crisis and Devonian-Carboniferous Boundary. In *Devonian climate, sea level and evolutionary events*, eds. R.T. Becker, P. Königshof, and C.E. Brett. *Geological Society of London, Special Publications* 423: 355–386.

Berberian, M. 1983. The southern Caspian: a compressional depression floored by a trapped, modified oceanic crust. *Canadian Journal of Earth Sciences* 20: 163–183.

Berberian, M., and G.C.P. King. 1981. Towards a paleogeography and tectonic evolution of Iran. *Canadian Journal of Earth Sciences* 18: 210–265.

Bischoff, G. 1957. Die Conodonten-Stratigraphie des rheno-herzynischen Unterkarbons mit Berücksichtigung der *Wocklumeria*-Stufe und der Devon/Karbon-Grenze. *Abhandlungen des Hessischen Landesamtes für Bodenforschung* 19: 1–64.

Bozorgnia, F. 1973. Paleozoic foraminiferal biostratigraphy of Central and East Alborz Mountains, Iran. *National Iranian Oil Company, Geological Laboratories* 4: 1–185.

Branson, E.R. 1934. Conodonts from the Hannibal Formation of Missouri. *Missouri University Studies* 8: 301–343.

Branson, E.B., and M.G. Mehl. 1934. Conodonts from the Grassy Creek shale of Missouri. *Missouri University Studies* 8: 171–259.

Branson, E.B., and M.G. Mehl. 1941. New and little known Carboniferous conodont genera. *Journal of Paleontology* 15: 97–106.

Brenckle, P.L., M. Gaetani, L. Angiolini, and M. Bahrammanesh. 2009. Refinements in biostratigraphy, chronostratigraphy, and paleogeography of the Mississippian (Lower Carboniferous) Mobarak Formation, Alborz Mountains, Iran. *GeoArabia* 14: 43–78.

Brezinski, D.K., C.B. Cecil, and V.W. Skema. 2010. Late Devonian glacigenic and associated facies from the central Appalachian Basin, eastern United States. *Geological Society of America, Bulletin* 122: 265–281.

Brice, D., J. Lafuste, A.F. De Lapparent, J. Pillet, and I. Yassini. 1974. Étude de deux gisements paléozoïques (Silurien et Dévonien) de l'Elbourz oriental (Iran). *Annales de la Société Géologique du Nord* 93: 177–218.

Brice, D., J. Jenny, G. Stampfli, and F. Bigey. 1978. Le Devonian de l'Elbourz oriental: stratigraphie, paléontologie (brachiopodes et bryozoaires), paléogeographie. *Rivista Italiana di Paleontologia e Stratigrafia* 84: 1–56.

Caputo, M.V., J.G. de Melo, M. Streel, J.L. Isbell, and C. Fielding. 2008. Late Devonian and early Carboniferous glacial records of South America. *Geological Society of America, Special Papers* 441: 161–173.

Cole, D., P.M. Myrow, D.A. Fike, A. Hakim, and G.E. Gehrels. 2015. Uppermost Devonian (Famennian) to Lower Mississippian events of the western US: Stratigraphy, sedimentology, chemostratigraphy, and detrital zircon geochronology. *Palaeogeography, Palaeoclimatology, Palaeoecology* 427: 1–19.

Cooper, C.L. 1939. Conodonts from a Bushberg-Hannibal horizon in Oklahoma. *Journal of Paleontology* 13: 379–422.

Coquel, R., S. Loboziak, G. Stampfli, and B. Stampfli-Vuille. 1977. Palynologie du Dévonien supérieur et du Carbonifère inférieur dans l'Elburz oriental (Iran nord-est). *Revue de Micropaléontologie* 20: 59–71.

Corradini, C., C. Spalletta, A. Mossoni, H. Matyja, and D.J. Over. 2016. Conodonts across the Devonian/Carboniferous boundary: a review and implication for the redefinition of the boundary and a proposal for an updated conodont zonation. *Geological Magazine* 154: 888–902.

Davoudzadeh, M. 1997. Iran. In *Encyclopedia of European and Asian regional geology*, eds. E.M. Moores and R.W. Fairbridge, 384–405. Dordrecht: Chapman and Hall.

Dreesen, R., and M. Orchard. 1974. "Intraspecific" morphological variation within *Polygnathus semicostatus* Branson and Mehl, In *Micropaleontological limits from Emsian to Visean. International Symposium on Namur 1974*, eds. J. Bouckaert, and M. Streel. *Geological Survey of Belgium, Publication* 21: 1–10.

Druce, E. 1969. Devonian and Carboniferous conodonts from the Bonaparte Gulf Basin, northern Australia and their use in international correlation. *Bureau of Mineral Resources* 98: 1–242.

Dzik, J. 2006. The Famennian "Golden Age" of conodonts and ammonoids in the Polish part of the Variscan Sea. *Palaeontologia Polonica* 63: 1–359.

Epstein, A.G., J.B. Epstein, and L.D. Harris. 1977. Conodont color alteration—an index to organic metamorphism. *US Geological Survey, Professional Paper* 995: 1–27.

Falahatgar, M., and H. Mosaddegh. 2012. Microfacies and palaeoenvironments of the Lower Carboniferous Mobarak Formation in the Kiyasar section, Northern Iran. *Boletín del Instituto de Fisiografía y Geología* 82: 9–20.

Falahatgar, M., A. May, and M. Sarfi. 2018. First report of the rugose coral *Hexagonaria davidsoni* from the Khoshyeilagh Formation (Devonian), Alborz Mountains, Northeastern Iran. *Boletín de la Sociedad Geológica Mexicana* 70: 787–795.

Fielding, C.R., T.D. Frank, L.P. Birgenheier, M.C. Rygel, A.T. Jones, and J. Roberts. 2008. Stratigraphic imprint of the Late Paleozoic Ice Age in eastern Australia: a record of alternating glacial and nonglacial climate regime. *Journal of the Geological Society of London* 165: 129–140.

Ghavidel-Syooki, M. 1994. Biostratigraphy and paleo-biogeography of some Paleozoic rocks at Zagros and Alborz Mountains. In *Treatise on the Geology of Iran, 18*, ed. A. Hushmandzadeh, 1–168. Tehran: Geological Survey of Iran.

Ghavidel-Syooki, M., and B. Owens. 2007. Palynostratigraphy and palaeogeography of the Padeha, Khoshyeilagh, and Mobarak formations in the eastern Alborz Range (Kopet-Dagh region), northeastern Iran. *Revue de Micropaléontologie* 50: 129–144.

Golonka, J. 2002. Plate-tectonic maps of the Phanerozoic. In *Phanerozoic reef patterns*, eds. W. Kiessling, E. Flügel, and J. Golonka. *SEPM Special Publication* 72: 21–75.

Golonka, J. 2007. Late Triassic and Early Jurassic palaeogeography of the world. *Palaeogeography, Palaeoclimatology, Palaeoecology* 244: 297–307.

Habibi, T., C. Corradini, and M. Yazdi. 2008. Conodont biostratigraphy of the Upper Devonian-Lower Carboniferous Shahmirzad section, central Alborz, Iran. *Geobios* 41: 763–777.

Hamdi, B., and P. Janvier. 1981. Some conodonts and fish remains from Lower Devonian (lower part of the Khoshyeylaq Formation) north east Shahrud, Iran. *Geological Survey of Iran, Report* 49: 195–210.

Haq, B.U., and S.R. Shutter. 2008. A chronology of Paleozoic sea-level changes. *Science* 322: 64–68.

Hartenfels, S. 2011. Die globalen *Annulata*-Events und die Dasberg-Krise (Famennium, Oberdevon) in Europa und Nord-Afrika—hochauflösende Conodonten-Stratigraphie, Karbonat-Mikrofazies, Paläoökologie und Paläodiversität. *Münstersche Forschungen zur Geologie und Paläontologie* 105: 17–527.

Hashemi, H. 2011. Vascular cryptogam plants of the Khoshyeilagh Formation, northern Shahrud, eastern Alborz Ranges. *Journal of Sciences, Islamic Republic of Iran* 22: 335–343.

Hass, W.H. 1959. Conodonts from the Chappel Limestone of Texas. *US Geological Survey, Professional Paper* 294: 365–399.

Helms, J. 1959. Conodonten aus dem Saalfelder Oberdevon (Thüringen). *Geologie* 8: 634–677.

Helms, J. 1961. Die "nodocostata-Gruppe" der Gattung *Polygnathus*. *Geologie* 10: 674–711.

Isaacson, P., J. Hladil, J. Shen, J. Kalvoda, and G. Grader. 1999. Late Devonian (Famennian) glaciation in South America and marine offlap on other continents. *Abhandlungen der Geologischen Bundesanstalt* 54: 239–258.

Isaacson, P., E. Diaz-Martinez, G.W. Grader, J. Kalvoda, O. Babek, and F.X. Devuyst. 2008. Late Devonian–earliest Mississippian glaciation in Gondwanaland and its biogeographic consequences. *Palaeogeography, Palaeoclimatology, Palaeoecology* 268: 126–142.

Jenny, J.G. 1977. *Géologie et stratigraphie de l'Elburz orientale entre Aliabad et Shahrud, Iran,* 1–238. Unpublished PhD dissertation, Université de Genève.

Jeppsson, L., and R. Anehus. 1995. A buffered formic acid technique for conodont extraction. *Journal of Paleontology* 69: 790–794.

Ji, Q., and W. Ziegler. 1993. The Lali section: an excellent reference section for Late Devonian in south China. *Courier Forschungsinstitut Senckenberg* 157: 1–183.

Kaiser, S.I., R.T. Becker, C. Spalletta, and T. Steuber. 2009. High-resolution conodont stratigraphy, biofacies and extinctions around the Hangenberg Event in pelagic successions from Austria, Italy and France. *Palaeontographica Americana* 63: 97–139.

Kaiser, S.I., R.T. Becker, T. Steuber, and Z.S. Aboussalam. 2011. Climate-controlled mass extinctions, facies, and sea-level changes around the Devonian/Carboniferous boundary in the eastern Anti-Atlas (SE Morocco). *Palaeogeography, Palaeoclimatology, Palaeoecology* 310: 340–364.

Kaiser, S.I., M. Aretz, and R.T. Becker. 2016. The global Hangenberg Crisis (Devonian–Carboniferous transition): review of a first-order mass extinction. In *Devonian climate, sea level and evolutionary events*, eds. R.T. Becker, P. Königshof, and C.E.

Brett. *Geological Society of London, Special Publications* 423: 387–437.
Klapper, G., and W. Ziegler. 1980. Devonian conodont biostratigraphy. In *The Devonian system*, eds. M.R. House, C.T. Scrutton, and M.G. Bassett. *Special Papers in Palaeontology* 23: 199–224.
Königshof, P., A. Bahrami, and S.I. Kaiser. 2021. Devonian/Carboniferous boundary sections in Iran. *Palaeobiodiversity and Palaeoenvironments* 101: 613–632.
Lakin, J.A., J.E.A. Marshall, I. Troth, and I.C. Harding. 2016. Greenhouse to icehouse: a biostratigraphic review of latest Devonian-Mississippian glaciations and their global effects. In *Devonian climate, sea level and evolutionary events*, eds. R.T. Becker, P. Königshof, and C.E. Brett. *Geological Society of London, Special Publications* 423: 439–467.
Lane, H.R., and W. Ziegler. 1983. Taxonomy and phylogeny of *Scaliognathus* BRANSON et MEHL, 1941 (Conodonta, Lower Carboniferous). *Senckenbergiana Lethaea* 64: 199–225.
Lane, H.R., C.A. Sandberg, and W. Ziegler. 1980. Taxonomy and phylogeny of some Lower Carboniferous conodonts and preliminary standard post-*Siphonodella* zonation. *Geologica et Palaeontologica* 14: 117–164.
Lasemi, Y. 2001. *Facies analysis, depositional environments and sequence stratigraphy of the Upper Pre-Cambrian and Paleozoic rocks of Iran*. Tehran: Geological Survey of Iran. (in Persian).
McGhee, G.R., M.E. Clapham, P.M. Sheehan, D.J. Bottjer, and M.L. Droser. 2013. A new ecological-severity ranking of major Phanerozoic biodiversity crises. *Palaeogeography, Palaeoclimatology, Palaeoecology* 370: 260–270.
Mehl, M.G., and L.A. Thomas. 1947. Conodonts from the Fern Glen of Missouri. *Journal of Science, Laboratory of Denison University* 40: 3–20.
Mosaddegh, H. 2000. *Microfossils, microfacies, sedimentary environment and sequence stratigraphy of the Mobarak Formation in Central Alborz,* 1–269. Unpublished PhD thesis, Tehran Teacher Training University.
Müller, K.J. 1956. Zur Kenntnis der Conodonten-Fauna des europäischen Devons, 1; Die Gattung *Palmatolepis*. *Abhandlungen der Senckenbergischen Naturforschenden Gesellschaft* 494: 1–70.
Munkhjargal, A., P. Königshof, S. Hartenfels, U. Jansen, A. Nazik, S.K. Carmichael, J.A. Waters, S. Gonchigdorj, C. Crônier, A. Yarinpil, O. Paschall, and A. Dombrowski. 2021. The Hushoot Shiveetiin gol section (Baruunhuurai Terrane, Mongolia): sedimentology and facies from a Late Devonian island arc setting. *Palaeobiodiversity and Palaeoenvironments*. https://doi.org/10.1007/s12549-020-00445-0.
Muttoni, G., M. Mattei, M. Balini, A. Zanchi, M. Gaetani, and F. Berra. 2009. The drift history of Iran from the Ordovician to the Triassic. In *South Caspian to Central Iran Basins*, eds. M.-F. Brunet, M. Wilmsen, and J.W. Granath. *Geological Society of London, Special Publications* 312: 8–29.
Myrow, P.M., J. Ramezani, A.E. Hanson, S.A. Bowring, G. Racki, and M. Rakociński. 2014. High-precision U-Pb age and duration of the latest Devonian (Famennian) Hangenberg event, and its implications. *Terra Nova* 26: 222–229.
Parvizi, T., A. Bahrami, P. Königshof, and S.I. Kaiser. 2021. Conodont biostratigraphy of Upper Devonian-Lower Carboniferous deposits in eastern Alborz (Mighan section), North Iran. *Palaeoworld*. https://doi.org/10.1016/j.palwor.2021.01.008.
Perri, M.C., and C. Spalletta. 1990. Famennian conodonts from clymenid pelagic limestone, Carnic Alps, Italy. *Palaeontographia Italica* 77: 55–83.
Pour, M.G., L.E. Popov, M. Omrani, and H. Omrani. 2018. The latest Devonian (Famennian) phacopid trilobite *Omegops* from eastern Alborz, Iran. *Estonian Journal of Earth Sciences* 67: 192–204.
Rhodes, F.H.T., R.L. Austin, and E.C. Druce. 1969. British Avonian (Carboniferous) conodont faunas and their value in local and intercontinental correlation. *Bulletin British Museum of Natural History (Geology), Supplement* 5: 1–313.
Rygel, M.C., C.R. Fielding, T.D. Frank, and L.P. Birgenheier. 2008. The magnitude of Late Paleozoic glacioeustatic fluctuations: a synthesis. *Journal of Sedimentary Research* 78: 500–511.
Salehirad, R., M. Alavi, J. Jenny, G. Stampfli, and M. Shahrabi. 1991. *Geological Quadrangle map of Iran. No H4, 1/250/000 Map of Gorgan.* Geological Survey of Iran. Tehran.
Sandberg, C.A., and R. Dreesen. 1984. Late Devonian icriodontid biofacies models and alternate shallow water conodont zonation. In *Conodont biofacies and provincialism*, ed. D.L. Clark. *Geological Society of America, Special Papers* 196: 143–178.
Sandberg, C.A., M. Streel, and R.A. Scott. 1972. Comparison between conodont zonation and spore assemblages at the Devonian-Carboniferous boundary in the western and central United States and in Europe. In *Septième Congrès International de Stratigraphie et de Géologie du Carbonifère, Krefeld, 23–28 August 1971. Compte Rendu, vol. 1,* 179–203. Krefeld: Geologisches Landesamt.
Sandberg, C.A., and W. Ziegler. 1973. Refinement of standard Upper Devonian conodont zonation based on sections in Nevada and West Germany. *Geologica et Palaeontologica* 7: 97–122.
Sandberg, C.A., and W. Ziegler. 1979. Taxonomy and biofacies of important conodonts of Late Devonian *styriacus*-Zone, United States and Germany. *Geologica et Palaeontologica* 13: 173–212.
Sandberg, C.A., W. Ziegler, K. Leuteritz, and S.M. Brill. 1978. Phylogeny, speciation and zonation of *Siphonodella* (Conodonta, Upper Devonian and Lower Carboniferous). *Newsletters on Stratigraphy* 7: 102–120.
Sandberg, C.A., J.R. Morrow, and W. Ziegler. 2002. Late Devonian sea-level changes, catastrophic events, and mass extinctions. *Geological Society of America, Special Papers* 356: 473–487.
Sannemann, D. 1955a. Oberdevonische Conodonten (to II). *Senckenbergiana Lethaea* 36: 123–156.
Sannemann, D. 1955b. Beitrag zur Untergliederung des Oberdevons nach Conodonten. *Neues Jahrbuch für Geologie und Paläontologie, Abhandlungen* 100: 324–331.
Sardar Abadi, M., E.I. Kulagina, D.F. Voeten, F. Boulvain, and A.C. Da Silva. 2017. Sedimentologic and paleoclimatic reconstructions of carbonate factory evolution in the Alborz Basin (northern Iran) indicate a global response to Mississippian (Tournaisian) glaciations. *Sedimentary Geology* 348: 19–36.
Scotese, C.R. 2001. *Atlas of Earth-History. Paleogeography, vol. 1.* Arlington: Paleomap Project.
Sepkoski, J.J. 1996. Patterns of Phanerozoic extinction: a perspective from global data bases. In *Global events and event stratigraphy in the Phanerozoic*, ed. O.H. Walliser, 35–51. Berlin: Springer.
Spalletta, C., M.C. Perri, J. Over, and C. Corradini. 2017. Famennian (Upper Devonian) conodont zonation: revised global standard. *Bulletin of Geosciences* 92: 31–57.
Stampfli, G.M. 1978. *Étude géologique générale de l'Elburz oriental au S de Gonbad-e-Qabus Iran N-E*, 1–329. Unpublished PhD thesis, University of Geneva, Science Faculty.
Stöcklin, J. 1968. Structural history and tectonic of Iran: a review. *American Association of Petroleum Geologists Bulletin* 52: 1229–1258.
Streel, M., M.V. Caputo, S. Loboziak, and J.H.G. Melo. 2000. Late Frasnian–Famennian climates based on palynomorph analyses and the question of the Late Devonian glaciations. *Earth Science Reviews* 52: 121–173.
Streel, M., M.V. Caputo, S. Loboziak, J. Melo, and J. Thorez. 2001. Palynology and sedimentology of laminites and tillites from the latest Famennian of the Parnaíba Basin, Brazil. *Geologica Belgica* 3: 87–96.
Thompson, T.L., and L.D. Fellows. 1970. Stratigraphy and Conodont biostratigraphy of Kinderhookian and Osagean (lower

Mississippian) rocks of southwestern Missouri and adjacent areas. *Missouri Geological Survey and Water Resources, Resources, Report of Investigations* 45: 1–263.

Torsvik, T.H., and L.R.M. Cocks. 2004. Earth geography from 400 to 250 Ma: a palaeomagnetic, faunal and facies review. *Journal of the Geological Society* 161: 555–572.

Torsvik, T.H., and L.R.M. Cocks. 2013. Gondwana from top to base in space and time. *Gondwana Research* 24: 999–1030.

Vachard, D. 1996. Iran. In *The Carboniferous of the World, vol. 3,* eds. R. Wagner, C.F.W. Prins, and L.F. Granados, 489–521. Madrid: Instituto Tecnologico Geominero.

Valeryi, B., M. Falahatgar, B.B. Blodgett, M. Javidan, and T. Parvizi. 2018. Brachiopods from the Famennian (Khoshyeilagh Formation) of Damghan, Northern Iran. In *Fossil Record 6*, eds. S.G. Lucas, and R.M. Sullivan. *New Mexico Museum of Natural History and Science Bulletin* 79: 37–49.

Voges, A. 1959. Conodonten aus dem Unterkarbon I and II (Gattendorfia und Pericyclus-Stufe) des Sauerlandes. *Paläontologische Zeitschrift* 33: 266–314.

Walliser, O.H. 1996. Global events in the Devonian and Carboniferous. In *Global Events and Event Stratigraphy in the Phanerozoic*, ed. O.H. Walliser, 225–250. Berlin: Springer.

Webster, G.D., C. Maples, R. Mawson, and M. Dastanpour. 2003. A cladid-dominated Early Mississippian crinoid and conodont fauna from Kerman Province, Iran and revision of the glossocrinids and rhenocrinids. *Journal of Paleontology* 77: 1–36.

Webster, G.D., C.G. Maples, M. Yazdi, S. Marcus, and J.A. Waters. 2011. Early Pennsylvanian, Bashkirian, echinoderms from eastern Iran, a potential transitional fauna between Laurentia/Avalonia and the Paleotethys, and a Permian cromyocrinid from central Iran. *Palaeobiodiversity and Palaeoenvironments* 91: 1–61.

Weddige, K. 1984. Externally controlled late Paleozoic events of the Iran Plate. *Neues Jahrbuch für Geologie und Paläontologie, Abhandlungen* 168: 278–286.

Wendt, J., B. Kaufmann, Z. Belka, N. Farsan, and A.K. Bavandpur. 2005. Devonian/Lower Carboniferous stratigraphy, facies patterns and palaeogeography of Iran. Part II. Northern and Central Iran. *Acta Geologica Polonica* 55: 31–97.

Ziegler, W. 1960. Die Conodonten aus den Geröllen des Zechsteinkonglomerates von Rossenray (südwestlich Rheinberg/Niederrhein) mit Beschreibung einiger neuer Conodontenformen. *Fortschritte in der Geologie von Rheinland und Westfalen* 6: 391–405.

Ziegler, W. 1962. Taxionomie und Phylogenie oberdevonischer Conodonten und ihre stratigraphische Bedeutung. *Abhandlungen des Hessischen Landesamtes für Bodenforschung* 38: 1–166.

Ziegler, W. 1969. Eine neue Conodonten-Fauna aus dem höchsten Oberdevon. *Fortschritte in der Geologie von Rheinland und Westfalen* 17: 179–191.

Ziegler, W., and C.A. Sandberg. 1984. *Palmatolepis*-based revision of upper part of standard Late Devonian conodont zonation. In *Conodont biofacies and provincialism*, ed. D.L. Clark. *Geological Society of America, Special Paper* 196: 179–194.

Ziegler, W., and C.A. Sandberg. 1990. The Late Devonian Standard Conodont Zonation. *Courier Forschungsinstitut Senckenberg* 121: 1–115.

Ziegler, W., C.A. Sandberg, and R.L. Austin. 1974. Revision of *Bispathodus* group (Conodonta) in the Upper Devonian and Lower Carboniferous. *Geologica et Palaeontologica* 8: 97–112.